CHARGE DENSITY WAVES IN ALTERNATING SPINLESS FERMION LADDERS

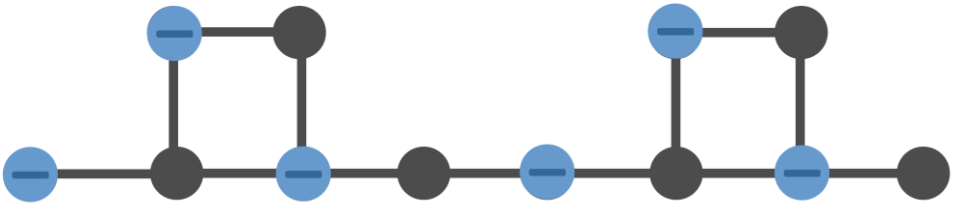

Alexander Fufaev

Institute of Theoretical Physics

Leibniz Universität Hannover

This thesis is submitted on 06/04/2023 for the degree of Master of Science

This document is the updated version (16/07/2023) of the original master thesis.

Author: Alexander Fufaev (fufaev@universaldenker.org)

Matriculation number: 3153800

Reviewer: Prof. Dr. Eric Jeckelmann

Second reviewer: Prof. Dr. Holger Frahm

Eigenständigkeits erklärung

Hiermit versichere ich, Alexander Fufaev, dass ich die Masterarbeit mit dem Titel „Charge density waves in alternating spinless fermion ladders“ selbst verfasst habe.

- Ich habe keine anderen als die angegebenen Quellen und Hilfsmittel benutzt.
- Alle wörtlich oder sinngemäß übernommenen Stellen der Arbeit aus anderen Quellen, wurden als solche gekennzeichnet.
- Die Masterarbeit wurde nicht in gleicher oder in ähnlicher Form einer anderen Prüfungsbehörde vorgelegt.

Unterschrift

Summary

Have you seen the picture on the cover of this master's thesis? That is the object of desire in this thesis and will not be studied until Chapter 4. It is a **spinless fermionic alternating ladder** with nearest neighbor interaction in a **C**harge **D**ensity **W**ave (CDW) phase. Say what? Don't worry, you will understand it after reading Chapter 1.

Spoiler alert! In this work, three quantum systems have been studied using the many-particle system solver **D**ensity **M**atrix **R**enormalization **G**roup (DMRG) algorithm:

1. A one-dimensional spinless fermionic chain - **1DSF chain**.
2. Two interacting 1DSF chains - **2-leg ladder**.
3. A ladder that an engineer would probably never be able to build - **1221 ladder**.

The main focus of this work is to **determine the phase transition** to the CDW phase in an *infinite* system, using the observables of a *finite* system. For the 1DSF chain and 2-leg ladder, one can compare the *numerically* determined phase transition with the *exact* phase transition predicted by theory. If the two do not match, then one can discard the method or observable used to determine the exact phase transition. In this way, **good methods and observables** were found **to predict a phase transition** in a 1DSF chain with an accuracy below 3%!

During the process, a method was discovered that could **assist in the search for phase transitions** in a wide variety of systems - the **P**hase **I**ndependent **F**it method (explained in Chapter 1.7.4). It not only provides an accurate prediction for the critical value in the 1DSF chain, but **can in principle be applied to different systems and their observables**. This is demonstrated in this work. Using this (and other methods), it was possible to **determine** the **theoretically unknown transition** to the CDW phase of the 1221 ladder. However, not everything is as bright as it seems. Some **unsolved problems** emerged, which could be interesting for theorists, computational physicists and of course for other students.

List of Abbreviations and Acronyms

CCS	**C**harge **C**onjugation **S**ymmetry
CDW	**C**harge **D**ensity **W**ave.
1DSF	One-**D**imensional **S**pinless **F**ermions.
DMRG	**D**ensity **M**atrix **R**enormalization **G**roup.
E_{p}	Single-particle gap.
ΔE	Excitation gap (difference between two lowest energy eigenvalues).
$F(x)$	Density-density correlation function.
K	Luttinger-liquid parameter.
S	(Von Neumann) bipartite entanglement entropy.
c	Central charge.
δ	(CDW) order parameter.
σ^2	Density fluctuation.
L	Length of the chain or ladder. In the case of a 1DSF chain or 1221-ladder L is the number of sites.
V_{cdw}	Exact critical value for Coulomb interaction indicating the phase transition to the CDW phase: $V_{\mathrm{cdw}} = 2$ (1DSF) and $V_{\mathrm{cdw}} = 0$ (2-leg).
V_{c}	Critical value of the Coulomb interaction determined with DMRG, suggesting a phase transition.

V_{err}	The most dominant error in the determination of V_{c}.
$V, V_{\mathrm{x}}, V_{\mathrm{y}}$	Coulomb interaction strength between nearest-neighbor fermions in x or y direction. In this work: $V := V_{\mathrm{x}} = V_{\mathrm{y}}$.
$t, t_{\mathrm{x}}, t_{\mathrm{y}}$	Hopping amplitudes between nearest-neighbor sites in x and y direction. In this work: $t := t_{\mathrm{x}} = t_{\mathrm{y}} = 1$.
c_x	Annihilation operator for site x.
$c_x^\dagger$	Creation operator for site x.
O	An arbitrary observable. Do not confuse with the Lanau symbol $\mathcal{O}$.

1. INTRODUCTION

1.1. ONE-DIMENSIONAL INTERACTING SYSTEMS

From a *theoretical* perspective, **one-dimensional interacting systems** are a fascinating area of study as the Fermi liquid theory fails to capture their behavior[1]. These systems require a new approach utilizing a different one-dimensional field theory, such as the **L**uttinger **L**iquid theory for metals, making them theoretically exceptional. In this work, one-dimensional **finite spinless fermionic systems** are studied and an attempt is made to make predictions about these systems in the thermodynamic limit. Some systems, such as a one-dimensional spinless fermionic chain (1DSF) can be solved exactly in the thermodynamic limit using the **Bethe ansatz**.[1,2] This allows for a comparison of exact results with numerical ones, as done in this work. In this way, not only the **theory can be tested**, but also the **usefulness of the numerical algorithms** to solve such theories.

Not only are these systems fascinating theoretically, but quasi-1d systems are also intriguing from an *experimental* standpoint. These systems **occur in nature** in the form of quantum chains, nanotubes, and edge states in the quantum Hall effect. Furthermore, quantum chains have the potential to **revolutionize technology miniaturization**. To harness this potential, it is essential to understand the transport mechanisms in quantum chains, as well as the interactions between chains and between fermions within a single chain.

In this work, the last two problems are investigated - the interaction between (spinless) fermions within a **1DSF chain**, the interaction of two 1DSF chains (**2-leg ladder**), and

interaction of fermions inside an **alternating 1221-ladder** (as shown on the cover of this thesis). These one-dimensional interacting systems are the most elementary systems that contain complex phenomena such as the **L**uttinger **L**iquid (LL) phase, **C**harge **D**ensity **W**ave (CDW) phase, and **phase separation**[1]. Despite their apparent simplicity, simulating spinless fermionic systems poses challenges. One of these challenges, which this work addresses, is the **precise identification of phase transitions**. As an example, the phase transition between the LL phase and CDW phase in the thermodynamic limit of a 1D spinless fermionic chain, which is well-known in theory, is difficult to pinpoint using numerical methods due to an **essential singularity**.[3] Such singularities at phase transitions make 1d systems a captivating subject of research. In fact, current studies are being conducted on various 1d systems and their modifications such as 2-leg ladders, alternating ladders, and wires on a substrate, to name a few[3–6]. Despite the essential singularity in the 1DSF chain, there are **several methods to determine the critical point** from the numerical data for a finite chain. These methods are presented in Chapter 1.6.

However, the 1D spinless fermionic chain (but also the 2-leg ladder) serves only as a toy model in this work, with which different methods for extracting critical points are tested and compared against exact results. It becomes much more interesting when investigating the **1221 ladder**, because here the **phase transitions are theoretically unknown**. Therefore, the best methods that worked for the 1DSF chain and 2-leg ladder are applied to the 1221 ladder to detect phase transitions.

1.2. DMRG: Algorithm to solve the many particles Hamiltonian

In this work, spinless fermionic systems are studied whose number of lattice sites is so large that the ground state of the system cannot be calculated *exactly* by any supercomputer in the world. This is because the dimension of the Hilbert space in which the ground state of the system lives grows *exponentially* with the system size. This exponential growth of the dimension also leads to the exponential growth of the required memory and CPU time[7]. Already the exact description of a system with twenty sites needs a Hilbert space with a dimension over one million. An exact computation of the ground state of larger systems is practically impossible, but also not necessary, because - at least in the case of one-dimensional systems - an approximation of the ground state by using of a suitable algorithm already provides a good overlap with the exact ground state[7].

In this work, the exact ground state is *approximated* using the **D**ensity **M**atrix **R**enormalization **G**roup (**DMRG**) algorithm. In the following, its principle is explained using a one-dimensional chain.

The used DMRG algorithm consists of two parts: **infinite DMRG** and **finite DMRG**. With the infinite DMRG, a chain is *built* recursively up to a **desired length** L and the dimension of the Hilbert space is *truncated* to a fixed maximal value m^2 to avoid the exponential growth. With the finite DMRG, which is executed after the infinite DMRG, the accuracy of the ground state is *improved* at fixed length.[8]

Basic objects for DMRG are[9]:

- Lattice site
- **Left block** $B_L(l,m)$ and **right block** $B_\mathrm{R}(l,m)$
- **Superblock** $B_\mathrm{S}(L',m^2)$ with L' as the number of sites.

A lattice site is described by two possible states: State $|1\rangle$ describes a state *occupied* by a spinless fermion and $|0\rangle$ an *unoccupied* state. The left block $B_\mathrm{L}(l,m)$ represents a part of the chain with **site** $1,\dots,l$ and the associated Hilbert space $\mathcal{H}_\mathrm{L}(l,m)$ is spanned by m **basis vectors** $|b_1\rangle,\dots,|b_m\rangle$. It is analogous for the right block: $B_\mathrm{R}(l,m)$. For the *exact* description of the block with spinless fermions, $m=2^l$ basis vectors are required. The superblock $B_\mathrm{S}(L',m^2)$ consists of the left and right block and represents the *whole* chain of length L'.

1.2.1. Infinite DMRG

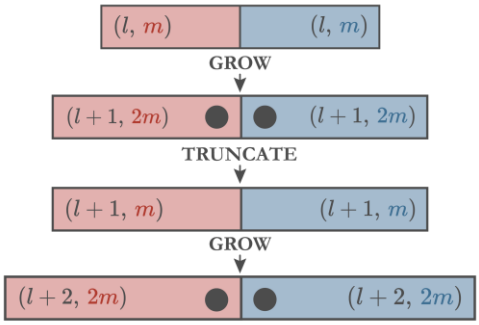

Figure 1.1: Basic principle of infinite DMRG.

The **infinite DMRG** starts with a left block $B_\mathrm{L}(l,m)$ and an equally sized right block $B_\mathrm{R}(l,m)$, each describing half of the superblock $B_\mathrm{S}(L',m^2)$, which has length $L'=2l$ and dimension m^2 and whose ground state can be calculated *exactly*. The two blocks are each increased by one lattice site in the next step: $B_\mathrm{L}(l+1,2m)$ and $B_\mathrm{R}(l+1,2m)$ (these new

blocks are called **enlarged blocks**). As a result, the dimension of the Hilbert space of the blocks is *doubled*. Adding one more site *quadruples* the original dimension m, so the dimension of the blocks grows exponentially with each additional site. After increasing the block size by one, infinite DMRG truncates the dimension back to the value m (see Figure 1.1).

How does the truncation process work? First, the new superblock Hamiltonian $H_S(2l + 2, 4m^2)$ has now two more sites as well as quadrupled dimension and is exactly diagonalized using **Davidson's algorithm** to obtain the **ground state** $|E_0\rangle$ of the system. The ground state is given by the tensor product of the basis vectors $|b_i\rangle$ and $|b_j\rangle$ of the left and right block[8]:

$$|E_0\rangle = \sum_{i=1}^{2m} \sum_{j=1}^{2m} a_{ij} |b_i\rangle \otimes |b_j\rangle \tag{1.1}$$

From the ground state, the **reduced density matrix** ρ_L of the left block (L stands for left) is calculated

$$(\rho_{ik})_L = \sum_{j=1}^{2m} a_{ij} a_{kj}^* \tag{1.2}$$

and exactly diagonalized to obtain their **eigenstates** $\{|w_\alpha\rangle,\ \alpha = 1, \dots, 2m\}$ and **eigenvalues** $\{w_\alpha\}$.[8] The eigenstates now serve as a *new basis* with which the Hamiltonian $H_L(l + 1, 2m)$ of the left block is represented.

Next, all states $|w_\alpha\rangle$ with the *smallest* probability w_α are removed from the new basis and only m states are kept in the basis. Omitting less probable states results in an *error* that indicates how severe the deviation of the *effective* ground state $|E_0\rangle$ will be from the *exact* ground state $|E_{0,\text{exact}}\rangle$. This error is called **discarded weight** ε and is calculated as follows:

$$\varepsilon = 1 - \sum_{\alpha=1}^{m} w_\alpha \tag{1.3}$$

The kept m basis states form the rows of an $m \times 2m$ operator P. With this operator the left block Hamiltonian $H_L(l + 1, 2m)$ is represented in the new effective basis:

$$H_L(l + 1, m) = P H_L(l + 1, 2m) P^\dagger \tag{1.4}$$

The effective Hamiltonian $H_{\mathrm{L}}(l+1,m)$ obtained by the transformation (1.4) is now described by a smaller $m \times m$ matrix instead of a $2m \times 2m$ matrix. Similarly, the right block and all other operators are transformed into the simplified basis. This transformation of the operators **into the eigenbasis of the reduced density matrix of the left block** represents the **truncation process**.

The two effective Hamiltonians $H_{\mathrm{L}}(l+1,m)$ and $H_{\mathrm{R}}(l+1,m)$ are used to construct the **effective superblock Hamiltonian**[9] $H_{\mathrm{S}}(2l+2,m^2)$, which now describes a chain with two more lattice sites, but has only $m^2 \times m^2$ matrix entries (rather than $4m^2 \times 4m^2$).

Then the left $B_{\mathrm{L}}(l+1,m)$ and right block $B_{\mathrm{R}}(l+1,m)$ are again each extended by one site, which doubles the dimension of each block: $B_{\mathrm{L}}(l+2,2m)$ and $B_{\mathrm{R}}(l+2,2m)$. Then the truncation process is applied again to undo this doubling: $B_{\mathrm{L}}(l+2,m)$ and $B_{\mathrm{R}}(l+2,m)$. Adding sites and truncating the Hilbert space is performed until a superblock of **desired length** L and **dimension** $(4m)^2$ is constructed.

Once the infinite DMRG has built up a chain length L, the approximated **ground state** $|E_0\rangle$ of the chain and its approximated **ground state energy** E_0 can be obtained by diagonalizing the final superblock Hamiltonian. In this ground state, the **mean value of a (local) observable** $\langle \hat{O}_i \rangle$ acting on the i-th site can then be calculated:

$$\langle \hat{O}_i \rangle = \langle E_0 | \hat{O}_i | E_0 \rangle = \sum_{\alpha=1}^{m} w_\alpha \langle w_\alpha | \hat{O}_i | w_\alpha \rangle \tag{1.5}$$

For more on the measurement of local and non-local observables (such as correlation functions), see the paper by A.L. Malvezzi[9].

1.2.2. Finite DMRG

The infinite DMRG always divided the superblock into two blocks of *equal length*. All bipartitions of *non-equal* block length, for example $B_{\mathrm{L}}(L/3,m)$ and $B_{\mathrm{R}}(2L/3,m)$, were ignored. The **finite DMRG** is used to iterate through different bipartitions of the chain so that the ground state energy (and any other observable) of a finite-length chain is made as precise as possible (for fixed m)[8].

Once the **desired chain length** L has been obtained using infinite DMRG, it will *not be changed* during finite DMRG.

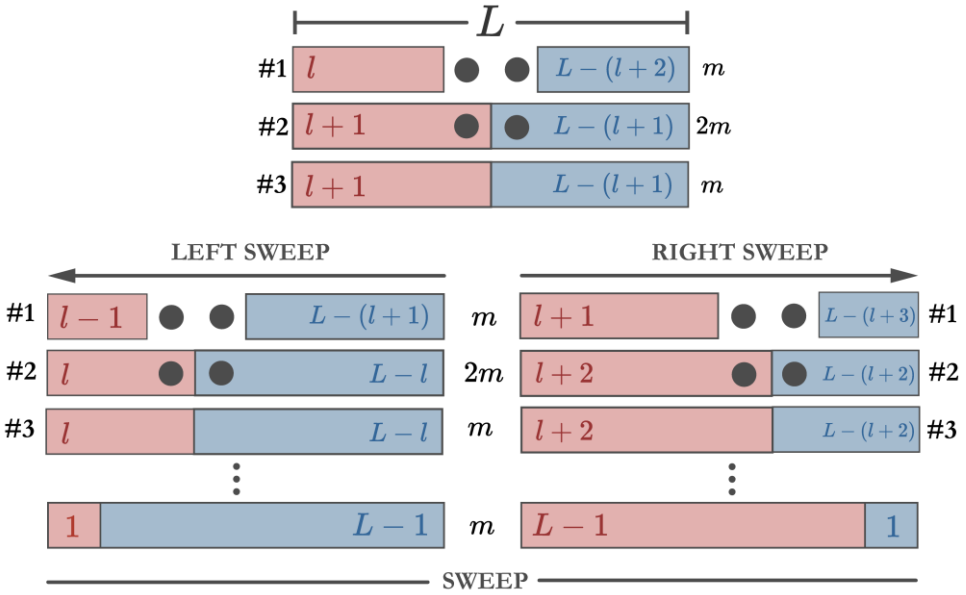

Figure 1.2: Basic principle of finite DMRG.

Here is a brief explanation of how finite DMRG works (see Figure 1.2): The finite DMRG starts with an effective superblock $B_S(L, m^2)$ of a fixed length L.

1) In the first step the superblock is divided into left $B_L(l, m)$ and right block $B_R(L - l - 2, m)$. Also, two sites are needed for the next step.
2) In the next step, the two single sites are integrated tensorially into left and right block, respectively. In this way the dimension of the blocks is doubled and they become larger by one site each: $B_L(l + 1, 2m)$ and $B_R(L - l - 1, 2m)$. Then the two blocks are combined to form a superblock $B_S(L, 4m^2)$, whose Hamiltonian $H_S(L, 4m^2)$ is diagonalized using Davidson's algorithm, and the ground state of the superblock is obtained.
3) The two enlarged blocks $B_L(l + 1, 2m)$ and $B_R(L - l - 1, 2m)$ are again truncated to dimension m, in the same way as in infinite DMRG.

These three steps are repeated for a subsequent **left sweep**. Here, in the first step, the left block is *decreased by one site*: $B_L(l - 1, m)$ and the right block is *increased by one site*: $B_R(L - l - 1, m)$. After that, steps #2 and #3 follow analogously. The left sweep is performed until the left block consists of only one site: $B_L(1, 2)$ and the right block consists of all except one site: $B_R(L - 1, m)$.

During the **right sweep**, on the other hand, in the first step the right block is *decreased by one site*: $B_R(L - l - 3, m)$ and the left block is *increased by one site*: $B_L(l + 1, m)$. Otherwise,

the algorithm runs analogously to the left sweep until the right block consists of only one site: $B_{\mathrm{R}}(1,1)$ and the left block consists of all except one site: $B_{\mathrm{L}}(L-1,m)$.

After the left and right sweeps are done, finite DMRG has done a **sweep**. The more sweeps performed, the more accurate the ground state and all measured observables. How many sweeps are needed for the convergence of the ground state depends on the model considered and on the chosen number m of basis states[9].

How can the algorithm be applied to *two-dimensional* structures, such as a 2-leg ladder or an alternating ladder? For this purpose, a **DMRG path** is defined along the lattice in a certain way and the model is converted into a one-dimensional chain:

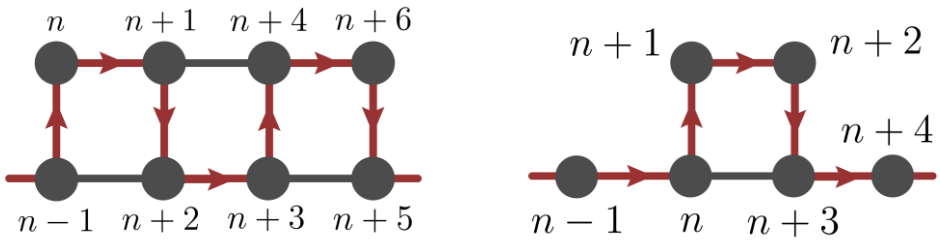

Figure 1.3: DMRG path for two different lattice structures. Left: 2-leg ladder. Right: Alternating 1221-ladder.

1.3. 1DSF CHAIN: HOW TO DESCRIBE 1D QUANTUM SYSTEM?

The following **tight-binding Hamiltonian** describes a one-dimensional many-particle system with L **sites** and **spinless fermions**:

$$H_{\mathrm{TB}} = -t \sum_{\langle ij \rangle} \left(c_i^\dagger c_j + \mathrm{H.c.} \right) \tag{1.6}$$

Here $c_i^\dagger$ *creates* a spinless fermion at site i of the chain and c_i *annihilates* a fermion at the same site. Since fermions have no spin degree of freedom, a lattice site can be occupied by *only one* fermion according to the **Pauli principle**.

Abbreviation **H.c.** stands for **H**ermitian **c**onjuagate of $c_i^\dagger c_j$ and the notation $\langle ij \rangle$ restricts the summation to *adjacent* lattice sites i and j. The **hopping parameter** $t \geq 0$ describes the hopping of a fermion from site i to the neighboring site j and vice versa. In all calculations t is set to one.

The Hamiltonian (1.6) describes a *noninteracting* chain for which the **ground-state energy** E_0 is known for any length L:

$$E_0(N, L, V = 0) = -2t \sum_{n=1}^{N} \cos\left(\frac{\pi n}{L+1}\right) \tag{1.7}$$

Here N is the **number of fermions** in the chain. The formula (1.7) is used later to compare with the numerically calculated ground state energy to check the correctness of the implementation of the DMRG program.

The Hamiltonian (1.6) becomes much more interesting if, in addition to the hopping term, an interaction term for neighboring sites is added:

$$H = -t \sum_{\langle ij \rangle} \left(c_i^\dagger c_j + \text{H.c.}\right) + V \sum_{\langle ij \rangle} c_i^\dagger c_i c_j^\dagger c_j \tag{1.8}$$

The Hamiltonian (1.8) is called the **spinless fermion model**. The additional term in the Hamiltonian accounts for the repulsion of the neighboring fermions. The repulsive **interaction parameter** $V \geq 0$ describes the strength of the repulsive Coulomb interaction between two neighboring fermions at the site i and j.

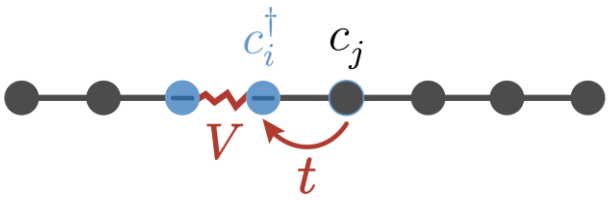

Figure 1.4: One-dimensional spinless fermion chain of length L with nearest neighbor repulsion and hopping.

There is an exact analytical solution for the 1DSF model, which is given by the **Bethe ansatz**[1,2]. The model is solved exactly for all L and therefore also **in the thermodynamic limit** ($L \to \infty$). The difficulty is to infer these results for an *infinite* chain from the numerical results for a *finite* chain.

In this work, only the case is considered where the system is **half filled** with fermions. Thus, a chain with *even* number of sites L is always filled with $N = L/2$ fermions and a ladder with $2L$ sites is always filled with $N = L$ fermions. Since *odd* 1DSF chains are also considered in this work, the number of fermions is *rounded off* in this case.

1.3.1. Quantum phase transition in 1D quantum systems

The model (1.7) or (1.8) has two parts that compete with each other. The hopping of the fermions from site to site is now made more difficult by the mutual repulsion. This leads to another phase which can occur in the 1DSF model.

Depending on the choice of the interaction parameter V, the ground state of (1.9) *in thermodynamic limit* ($L \to \infty$) is in one of the two phases:

1. **L**uttinger **L**iquid (**LL**) phase – this *metallic* quantum phase occurs when the interaction parameter V is smaller than or equal two.[1] In this phase, the density distribution of the fermions is uniform: $\langle c_x^\dagger c_x \rangle = \frac{1}{2}$.

2. **C**harge **D**ensity **W**ave (**CDW**) phase – this *insulating* quantum phase occurs when the Coulomb parameter V is greater than two[1]. In this phase, the repulsion of the fermions is so strong that they take the largest possible distance to each other. In the limit $V \gg 2$ the fermions occupy every second site and the density distribution oscillates with site x: $\langle c_x^\dagger c_x \rangle = \frac{1}{2} + (-1)^x \delta$. Here δ is the CDW order parameter and its magnitude $|\delta|$ takes the values in the interval $[0, \frac{1}{2}]$. The order parameter approaches $|\delta| \to 0.5$ for $V \to \infty$. The order parameter is discussed in more detail in Chapter 1.6.6.

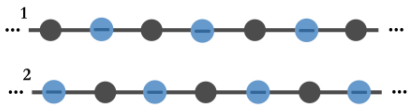

Figure 1.5: Two possible fermion arrangements that make the chain an insulator. The ground state $|E_0\rangle$ is degenerate in this CDW phase: $E_0 = E_1$.

Thus, there is a **quantum phase transition** at $V_{\mathrm{cdw}} = 2$ between the LL phase the CDW phase. One of the goals of this thesis is to investigate how this phase transition changes when we add another chain that interacts with the first one (**2-leg ladder**) and then what happens when the ladder is distorted (**alternating 1221-ladder**).

1.3.2. Particle-hole symmetry and open boundary conditions

In addition to the Hamiltonian (1.8), the following Hamiltonian, which has **particle-hole symmetry**, is also investigated[1]:

$$H' = -t \sum_{\langle ij \rangle} \left(c_i^\dagger c_j + \text{H.c.} \right) + V \sum_{\langle ij \rangle} \left(n_i - \frac{1}{2} \right) \left(n_j - \frac{1}{2} \right) \tag{1.9}$$

The two Hamiltonians (1.8) and (1.9) are equivalent for *periodic* boundary conditions up to a constant. For *open* boundary conditions, on the other hand, the two Hamiltonians differ not only by a constant, but also by the following **boundary term** (in the one-dimensional case):

$$\Delta\mathrm{CCS} = \frac{V}{2} (n_1 + n_L) \tag{1.10}$$

The ground state calculated with DMRG **converges better** when **open boundary conditions** are used[10]. This is the reason why *open* boundary conditions are used in this work. In the following:

- A system is **with CCS**, if the particle-hole symmetric Hamiltonian (1.9) = (1.8) + (1.10) is used. Here CCS stands for **C**harge **C**onjugation **S**ymmetry.
- A system is **without CCS** if the Hamiltonian (1.8) is used.

This boundary term ΔCCS will yield a different result for calculated observables depending on the parity of the chain. For an *odd* chain length, the two degenerate ground states $|E_0\rangle$ and $|E_1\rangle$, for example for $V \gg 2$, have a different number of particles: $N_0 = (L+1)/2$ and $N_1 = N_0 - 1$ so that one ground state occupies the chain with **two edge fermions** and the other ground state does not (see Figure 1.6).

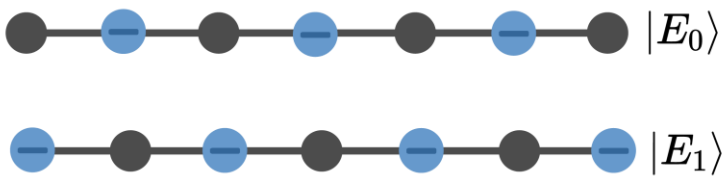

Figure 1.6: Different number of particles cancels the degeneracy of the ground state of an odd chain.

1.4. 2-LEG-LADDER: TWO INTERACTING 1DSF CHAINS

After examining a single chain, another chain is brought into interaction with the first chain. Two such coupled chains, as shown in Figure 1.7, form a **2-leg ladder**[11].

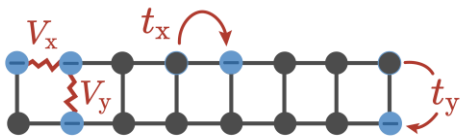

Figure 1.7: Homogeneous 2-leg ladder with $t_x = t_y = 1$ and $V_x = V_y$.

In this work, the hopping parameter along the chain t_x is equal to that between the chains: $t_x = t_y = 1$. Also, the repulsion between two neighboring fermions on *one* chain or on *different* chains is equal: $V_x = V_y$. The 2-leg ladder is described by the generally written Hamiltonians (1.8) and (1.9).

The **ground state energy** $E_0(L, N)$ of a *non-interacting* ladder ($V = 0$) of length L and with N fermions is the sum of the lowest **single-particle energies** ε_0:

$$\varepsilon_0(n_y, n_x) = (-1)^{n_y} + 2\cos\left(\frac{\pi n_x}{L+1}\right) \tag{1.11}$$

Here is $n_y \in \{0,1\}$ and $n_x \in \{1, \ldots, N\}$. The *exact* ground state energy $E_0(L, N)$ is used in Chapter 3 to be compared with the *numerical* ground state energy for $V = 0$.

The phase transition to the CDW phase for an *infinite* ladder already happens at $V_{cdw} = 0$.[1] Like the CDW phase of the 1DSF chain, the **CDW phase** of the 2-leg ladder is **twofold degenerate**. The two degenerate CDW ground states $|E_0\rangle$ and $|E_1\rangle$ for $V \gg 0$ are shown in Figure 1.8. Again, as with a chain, there is a difficulty of deducing the behavior of an *infinite* ladder from the results of a *finite* ladder.

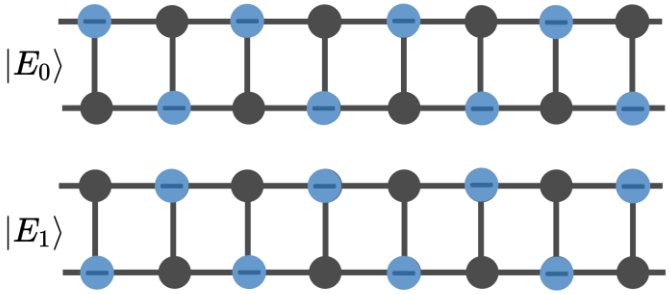

Figure 1.8: An infinite 2-leg ladder has a twofold degenerate ground state in the CDW phase. Shown is the arrangement of fermions for large V.

1.5. Alternating ladder: Distortion of a 2-leg-ladder

Next, lattice sites are removed as shown in Figure 1.9. The resulting structure is an *alternating* ladder, such as a **1221 ladder** in this case.

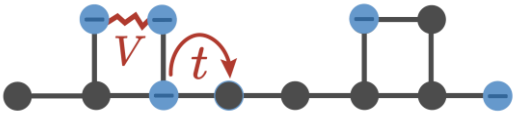

Figure 1.9: A 1221 ladder with alternating number of sites per rung.

In order for DMRG to be applied to the 1221 ladder, it is "flattened" into a chain. This is accomplished by choosing an arbitrary DMRG path along the 1221 ladder, which then represents a chain, as shown in Figure 1.3. Here, the Hamiltonians (1.8) and (1.9) contain hopping and interaction terms between the n-th and $(n+3)$-th lattice sites. To provide the 1221 ladder with CCS, the potential $-V/2$ is added to the fermions on sites n and $n+3$ and the potential $V/2$ is added to the ends $n = 1$ and $n = L$ of the chain. The number L of sites must be a multiple of six for a 1221 ladder to maintain the 1221 structure: $L = 6m$ with $m \in \mathbb{N}$.

For such an alternating ladder with interacting spinless fermions no exact phase transitions are known and it has not been investigated as far as I could research. Alternating ladders with similar structure and *with spin* have been studied by K. Essalah et al.[12]

1.6. THE INVESTIGATED OBSERVABLES

This chapter briefly introduces the studied observables, the theoretical expectations for an infinite chain, how they are calculated, and their physical interpretation.

The observables of the 1DSF chain are studied with an *even* and *odd* number of sites L. For a two-leg ladder and a 1221-ladder, only an *even* number of lattice sites can be considered. All three models are also simulated *with* and *without CCS*.

1.6.1. Entanglement entropy

The first observable to be studied is the **von Neumann entropy** S. It is defined as follows for a bipartite system divided into two blocks B_L and B_R, which in this work are of equal length[8]:

$$S = -\mathrm{Tr}[\rho_\mathrm{L} \ln(\rho_\mathrm{L})] = -\sum_{\alpha=1}^{m} w_\alpha \ln(w_\alpha) \tag{1.12}$$

Here, w_i are the **eigenvalues** of the **reduced density matrix** ρ_L of the ground state of the subsystem B_L of the chain. The entropy S describes how entangled the blocks B_L and B_R are with each other. $S = 0$ means that the blocks are not entangled at all. The entropy and thus the entanglement is maximal: $S = \ln(m)$ if all eigenvalues w_α are equal.

For a 1DSF chain, the entropy $S(L)$ is theoretically expected to behave logarithmically as a function of length L, for interaction potential $V \leq 2$ (as long as the entropy does not exhibit Friedel oscillations)[13]:

$$S(L) = \frac{c}{3} \ln\left(\frac{L}{\pi}\right) + a \tag{1.13}$$

Here, a and c are two constants that depend on the model under consideration. The constant c is special here, which is why it will be treated in a more detail in the next chapter. Eq. (1.13) also reveals how $S(V)$ as a function of V will behave for $V \leq 2$ in the limit $L \to \infty$: $S(V \leq 2)$ will diverge!

1.6.2. Central charge

The constant c, which appears in the formula (1.13) for entropy, is called **central charge** and it classifies different models which are conformally invariant according to the **C**onformal **F**ield **T**heory (**CFT**)[8,14].

In the *thermodynamic limit* of the 1DSF model, the function $c(V)$ shows a discontinuity at the critical point $V = 2$.[4] This discontinuity separates the metallic from the CDW phase:

- In the metallic phase $c(V \leq 2) = 1$.
- In the CDW phase $c(V > 2) = 0$.

There are two ways to determine the central charge numerically: By fitting the entropy with Eq. (1.13) or by looking at the difference of Eq. (1.13) for two different chain lengths L and L':

$$c(L, L') = 6 \cdot \frac{S(L) - S(L')}{\ln(L) - \ln(L')} \tag{1.14}$$

Eq. (1.14) can also be applied to the 2-leg ladder and 1221-ladder as long as the entropy exhibits logarithmic behavior (1.13).

1.6.3. Ground state energy

The **ground state energy** E_0 is the smallest eigenvalue of the considered Hamiltonian (1.8) or (1.9). In the CDW phase, the ground state of the infinite 1DSF chain is twofold degenerate: $|E_0\rangle = |1010\ldots\rangle$ and $|E_1\rangle = |0101\ldots\rangle$ with $E_0 = E_1$.

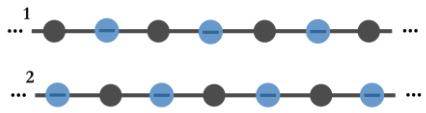

Figure 1.10: Two possible states of the infinite 1DSF chain leading to the twofold degeneracy of the ground state energy.

The ground state energy gives another possibility to choose a good value for m, at least for $V = 0$. For this purpose, the **deviation** $|E_0(m) - E_{0,\text{exact}}|$ of the **exact energy** $E_{0,\text{exact}}$, calculated with (1.7), from the **numerically calculated value** $E_0(m)$ as a function of $1/m$ is plotted. The value of m is chosen that gives a desired accuracy of the observable. This method is used in Figure 1.11 for different number of sweeps for a chain length $L = 500$.

The deviation does not change when the number of sweeps is increased starting from 4. The accuracy of the determination of the critical value $V_{\text{cdw}} = 2$ of the 1DSF model in this work is limited to 10^{-3}. Therefore, the **dimension** $m = 100$ is chosen, which gives a deviation $|E_0(m) - E_{0,\text{exact}}| \approx 10^{-4}$ (convergence error). This value is a good balance between the computation time and the accuracy of the calculations.

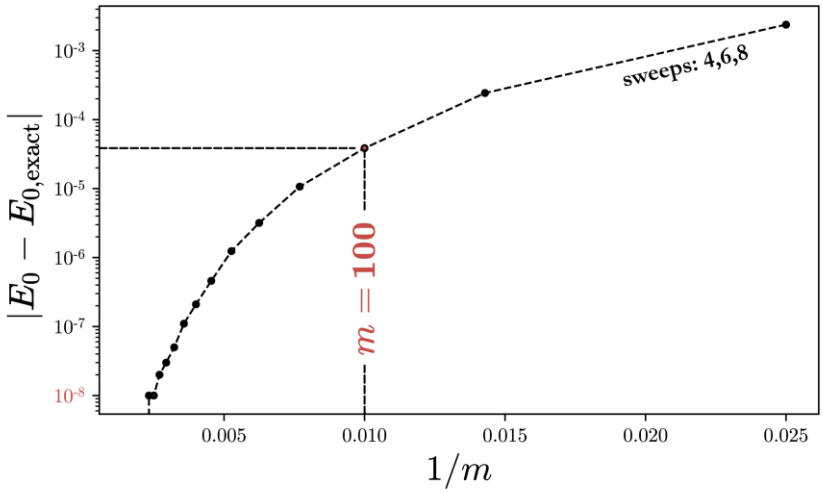

Figure 1.11: Deviation of the ground state energy $E_0(m)$ from the exact value $E_{0,\text{exact}}$ as a function of m for a non-interacting chain ($V = 0$) of length $L = 500$ for 4, 6 and 8 sweeps. Sweeps do not alter the curve.

1.6.4. Excitation gap

The **excitation gap** ΔE in this work is the difference between the smallest two energy eigenvalues E_1 and E_0 of the Hamiltonian (1.8) or (1.9):

$$\Delta E = E_1 - E_0 \tag{1.15}$$

In the LL phase ($V \leq 2$), the 1DSF chain is expected to behave like a metal and the energy gap ΔE *in the thermodynamic limit* vanishes. But also in the CDW phase ($V > 2$), the difference ΔE should be zero in the thermodynamic limit, since the ground state is *twofold degenerate*. For a *finite* chain, as can be seen in Chapter 2.3, the excitation gap is not zero everywhere!

1.6.5. Single-particle gap

Single-particle gap E_p describes the energy required to excite a single particle from the highest level below the Fermi level to the lowest level above the Fermi level[3].

$$E_\mathrm{p} = E_0(N+1) + E_0(N-1) - 2E_0(N) \tag{1.16}$$

Here, $E_0(N+1)$ is the ground state energy of the half-filled chain with one *additional* fermion and $E_0(N-1)$ is the ground state energy with one *less* fermion. Unlike the excitation gap ΔE, the single-particle gap E_p bypasses degeneracy and provides the actual difference in energy between the ground state and first excited state in the CDW phase. In the thermodynamic limit of a half-filled chain, the theory for the 1DSF model predicts the following behavior for the $E_\mathrm{p}(V)$ curve[1,3]:

- In the *metallic phase* $V \leq 2$ the gap vanishes.

- *Above the phase transition* $V = 2$, the gap opens exponentially.
- In the *CDW phase* for $V \gg 2$ the gap E_p approaches V.

1.6.6. CDW order parameter

The **CDW order parameter** δ is the alternating sum of the ground state particle densities and measures how well a CDW has formed. The CDW order parameter is defined as follows [4]:

$$\delta = \frac{1}{L}\sum_{x=1}^{L}(-1)^x\langle c_x^\dagger c_x\rangle \tag{1.17}$$

CDW order parameter lies in the range $0 \leq |\delta| \leq 0.5$ and the summation goes over all lattice sites. In the thermodynamic limit of a half-filled chain, the exact $\delta(V)$ curve for the 1DSF model behaves as follows.[3]:

- In the *metallic phase* $V \leq 2$ the CDW order parameter vanishes.
- In the *CDW phase* for $V > 2$ the magnitude $|\delta|$ increases monotonically with V and saturates towards the value $|\delta| \to 0.5$ for $V \to \infty$. The convergence of the order parameter $|\delta(V)|$ for $V > 4$ can be approximated by the following 2nd degree polynomial (the accuracy can be improved if higher order polynomials $\mathcal{O}(V^{-4})$ are included)[3]:

$$\delta\left(\frac{1}{V}\right) = A + B\left(\frac{1}{V}\right)^2 + \mathcal{O}(V^{-4}) \tag{1.18}$$

Here $A = 0.5$ and $B = -2$ are coefficients given by the theory for an infinite 1DSF chain. They are used as fit parameters in this work.

1.6.7. Density fluctuation

The **density fluctuation** σ^2 describes the average deviation of all ground state **particle densities** $\langle c_x^\dagger c_x\rangle = n_x$ from the **mean value** $N/L = 1/2$.

$$\sigma^2 = \frac{1}{L}\sum_{x=1}^{L}\left(\langle c_x^\dagger c_x\rangle - \frac{1}{2}\right)^2 \tag{1.19}$$

Because of the constant particle density $n_x = 1/2$ in the LL phase of an infinite chain, σ vanishes for $V \leq 2$. In the CDW phase, on the other hand, the particle density oscillates from lattice site to lattice site according to Eq. (1.17) and the density fluctuation has a finite value, becoming at most 1/4.

1.6.8. Correlation function and LL parameter

Density-density correlation functions $F(x - x_0)$ (also called **charge correlation function**) for a chain is defined as:[4]

$$F(x - x_0) = \langle n_{x_0} n_x \rangle - \langle n_{x_0} \rangle \langle n_x \rangle \tag{1.20}$$

The expectation values are calculated in the ground state $|E_0\rangle$ of the chain. As the name implies, $F(x - x_0)$ describes how the **site** x_0 *correlates* with another **site** x located at **distance** $x - x_0$. The **fixed point** x_0 is placed in the middle $x_0 = L/2$ of the 1DSF chain or at the edge $x_0 = 1$.

For a 1DSF chain in the Luttinger liquid phase ($V \leq 2$) *in the thermodynamic limit*, the **magnitude of the correlation function** $|F(x)|$ obeys a power law[4]:

$$|F(x)| = A|x|^{-2K} \tag{1.21}$$

Here A und K are two fit parameters, whereby the exponent K plays a special role here. It is called **Luttinger liquid parameter** and it is an indicator for the breakdown of the LL phase and thus the indicator for the transition to another phase. In the LL phase, $K(V)$ decreases from the value $K(0) = 1$ for a *non-interacting chain* with larger V until it reaches the value $K(V_{\text{cdw}}) = 1/2$ at the theoretical critical point $V_{\text{cdw}} = 2$ and initiates the breakdown of the LL phase[4]:

$$K(V) = \frac{\pi}{2} \frac{1}{\pi - \arccos(V/2\,t)} \tag{1.22}$$

This behavior of the LL parameter is exploited in Chapter 2.7 to determine the critical value of the 1DSF chain. It should also be mentioned that in the CDW phase ($V > 2$) of an infinite 1DSF chain, the density $\langle n_x \rangle$ is no longer constant and therefore the interpretation of the correlation function and the LL parameter becomes difficult. But even in a *finite* 1DSF chain in the metallic phase, the density $\langle n_x \rangle$ may fluctuate slightly, so that the correlation function may deviate from a perfect power law behavior (see Chapter 2.7).

1.7. THE 5 USED METHODS TO EXTRACT CRITICAL VALUE

This chapter presents **methods for determining the theoretical critical value V_{cdw}**, which indicates the point at which a phase transition occurs between the metallic and CDW phases. These methods are not limited to a specific observable or model. Some methods work for a single observable in a chain, while others can handle multiple observables in a chain or even work across different models.

1.7.1. Method #1: Discontinuity or Extremum in an Observable of a Finite System

In the first method, the critical value is extracted directly from the plot of the observable $O(V)$ of a *finite* system. The phase transition is revealed by a discontinuity or extremum in the $O(V)$ plot. This method can be applied to the central charge $c(V)$ of a 1DSF chain where it exhibits an extremum (see Chapter 2.2) or it can be applied to multiple observables of the 1221 ladder that show a discontinuity (see Chapter 4).

1.7.2. Method #2: Discontinuity or Extremum in an Observable of an Infinite System

The second method requires a little more work. As in the first method, the critical value is determined from the extremum or discontinuity of the function $O(V)$. However, for this, the observable must first be determined for an *infinite* chain: $O(V, L \to \infty)$. The method works as follows:

1. **Plot** the observable $O(1/L)$ as a function of the inverse length $1/L$ for different interaction parameters V.
2. **Fit** the observable $O(1/L)$ with a suitable function (usually a polynomial function up to 4th order) and **extrapolate** the function to the vertical axis intercept where $1/L = 0$. The intercept $O(V, 1/L = 0) \coloneqq O_\infty(V)$ with the vertical axis is then the extrapolated value of the observable for an *infinite* chain.
3. **Plot** the extracted axis intercepts $O_\infty(V)$ as a function of V and read off the extremum. The extremum is close to the phase transition.

The problem with this method is that the extremum only appears when a suitable fit function is used. An inappropriate choice of fit function and the method is useless. Another problem is that the observable $O(1/L)$ has a *different* functional behavior in the

different phases. Therefore, fitting both phases with a *single* function leads to a systematic error in one of the phases.

This method works well with the single-particle gap and partially with the excitation gap of a 1DSF chain.

1.7.3. Method #3: Exponential Fit Near Opening Gap

The third merthode is mainly tailored to the single-particle gap. According to the theory, the single-particle gap opens exponentially slowly near the phase transition[3] with $A = 16\pi$, $B = \pi^2/2$ and $V_c = V_{cdw} = 2$:

$$O(V) = A \exp\left(-\frac{B}{\sqrt{V - V_c}}\right) \tag{1.23}$$

Therefore, this behavior can be used to fit the single-particle gap, using A, B and V_c as fit parameters. From the fit of the region near the phase transition, the critical value V_c can be determined. To make the fit consistent the single-particle gap is **fitted between $\underline{V} = 2.1$ and $\overline{V} = 6$**.

Gebhard et al (2023) have determined the critical value very accurately by fitting the single-particle gap[3]. This method is applied in this work not only to single-particle gap, but also to excitation gap (see Chapters 2.3 and 2.4).

1.7.4. Method #4: Phase Independent Fit

To overcome the problem with the systematic error of the second method or the impossibility to extract the intercept with the vertical axis, this thesis postulates the following new method for extracting the critical value in thermodynamic limit: Consider a system with two or more phases. Calculate a suitable observable $O(L)$ for this system as a function of the system size L. Make a fit of $O(L)$ in the region $[\underline{L}, \overline{L}]$, where $O(L)$ exhibits the *same* functional behavior in *both* phases as shown in Figure 1.12.

As will be shown in the measurements, the fit with the *power law* is in many cases the *most universal* and the *most accurate*. Of course, other fit functions (for example a linear one) can also be tried. What is important here is that the chosen fit function should fit both phases equally well:

$$O(L) = \begin{cases} O'L + a \text{ (linear)} \\ aL^{\kappa} \text{ (power law)} \\ \text{something else} \end{cases} \tag{1.24}$$

Here O' is the derivative of $O(L)$ and used in this method just like a and κ as fit parameter.

The method in combination with the power law, works as follows:

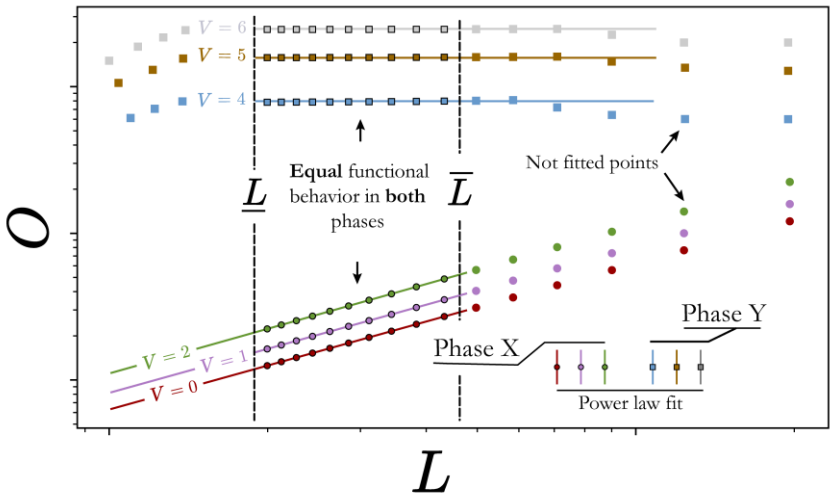

Figure 1.12: Find and fit equal functional behavior of an observable $O(L)$ in both phases X and Y. Power law behavior was found on a double logarithmic scale in both phases. This power law region inside $[\underline{L}, \overline{L}]$ is fitted for different V. The power law exponent $\kappa(V)$ could provide critical value for thermodynamic limit as a function of V.

1. **Plot** the observable $O(L)$ for different interaction parameters V on a double logarithmic scale. A power law behavior on a double logarithmic scale must result in a straight line.
2. **Find** the region of $O(L)$ for all V that behaves according to the power law and **fit** that region.
3. **Extract** the power law exponents κ of the fits for different V and **plot** $\kappa(V)$.
4. **Read off** the extremum of the function $\kappa(V)$. The extremum is near the phase transition and provides the critical value V_{cdw}.

1.7.5. Method #5: Intersection of an Observable with a Special Value

This method takes advantage of the fact that the function $O(V)$ crosses a certain value O_{int}, which is at the critical value V_c. This particular value O_{int} is predicted by theory. For example, LL theory predicts that when the LL parameter is $O_{\text{int}}(V_c) = K(V_c) = 0.5$, the LL phase breaks down and the interaction potential at this point is equal to the critical value V_c (see Chapter 2.2 and 2.7 for its application).

This method assumes that the model shows a LL phase and the LL parameter can be determined, for example, by using correlation functions.

2. RESULTS FOR 1DSF CHAIN

First, the 1DSF chain is investigated, where the critical value $V_{\mathrm{cdw}} = 2$ is known. Different observables are calculated for different parameters and it is checked how well the simulated results agree with the theoretical results and whether the critical value can be extracted from these results.

2.1. ENTANGLEMENT ENTROPY

Figure 2.1 shows the **entropy** $S(L)$ calculated with DMRG as a function of the **length** L and Figure 2.2 show the entropy $S(V)$ as a function of the **interaction potential** V for an *odd* chain *without* CCS.

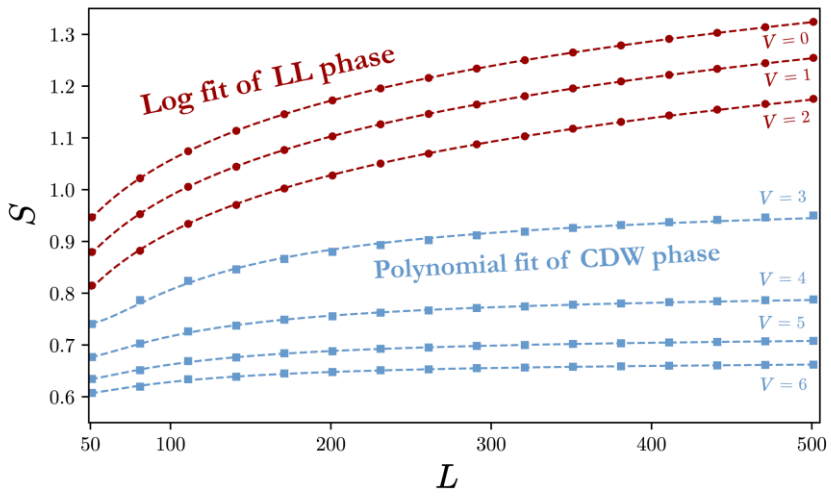

Figure 2.1: Entropy $S(L)$ of an odd chain length without CCS as a function of L for various interaction potentials V.

- **For V much smaller than 2**, the entropy $S(L)$ behaves *logarithmically* according to Eq. (1.13), and the entropy diverges with L, as predicted by the **C**onformal **F**ield **T**heory.
- **Near the phase transition $V \approx 2$**: The behavior is not clear. It could be logarithmic, but also polynomial. This, by the way, is the problem that is later avoided with the **P**hase **I**ndependent **F**it method.
- **For V much larger than 2**, the logarithmic fit is not suitable. The $S(L)$ data points are best fit with a *polynomial function* of 2nd order[3]:

$$S(L) = a_1 + \frac{a_2}{L} + \frac{a_3}{L^2} \tag{2.1}$$

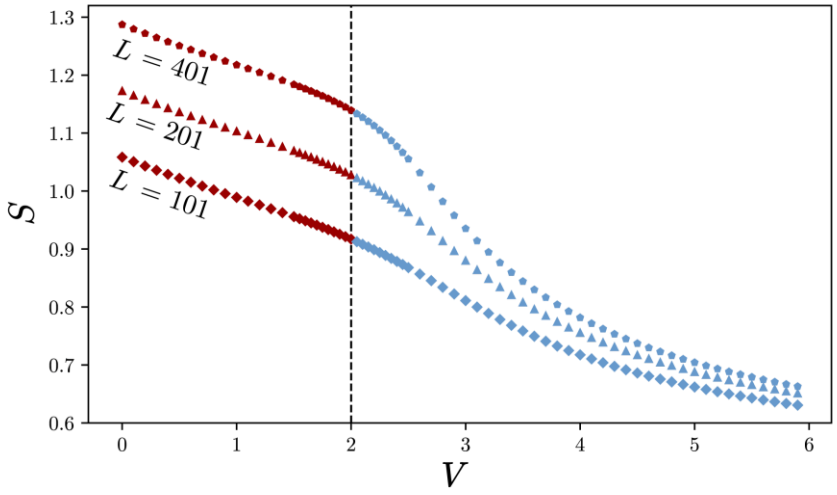

Figure 2.2: Entropy $S(V)$ of a 1DSF chain without CCS as a function of V for various lengths.

In the thermodynamic limit of the CDW phase, the entropy $S(V)$ as a function of V must have a constant value a_1 according to Eq. (2.1) and thus be independent of length. However, as Figure 2.2 shows, for an *odd* chain *without* CCS, this is only satisfied for a very large interaction potential V. This is also true for an *even* chain *with/without* CCS. For an *odd* chain *with* CCS, the entropy is already length independent starting at $V \approx 3$. Despite some differences depending on the parity of the chain length and CCS symmetry, all data points $S(L)$ show either logarithmic (1.13) or polynomial (2.1) behavior.

The extraction of the critical value $V_{\mathrm{cdw}} = 2$ from the entropy $S(V)$ seems to be impossible here, because the function $S(V)$ shows neither a discontinuity nor an extremum near $V \approx 2$. However, it is possible to apply method #1 to the **slope** $S'(V) = \Delta S/\Delta V$ of the entropy to obtain a definite result for the critical value.

As Figure 2.3 (inset) shows, the slope S' of the entropy has a **minimum** $S'(V_{\mathrm{min}})$ **at** V_{min}, which goes towards the critical value $V_{\mathrm{cdw}} = 2$ with the larger chain length, but

unfortunately does not reach it. A plot of $V_{\mathrm{min}}(L)$ as a function of length L shows that a larger length is necessary to best approximate the critical value. The best approximation V_c for the largest length investigated is listed in Table 2.1. This method provides only a rough estimate for the critical point.

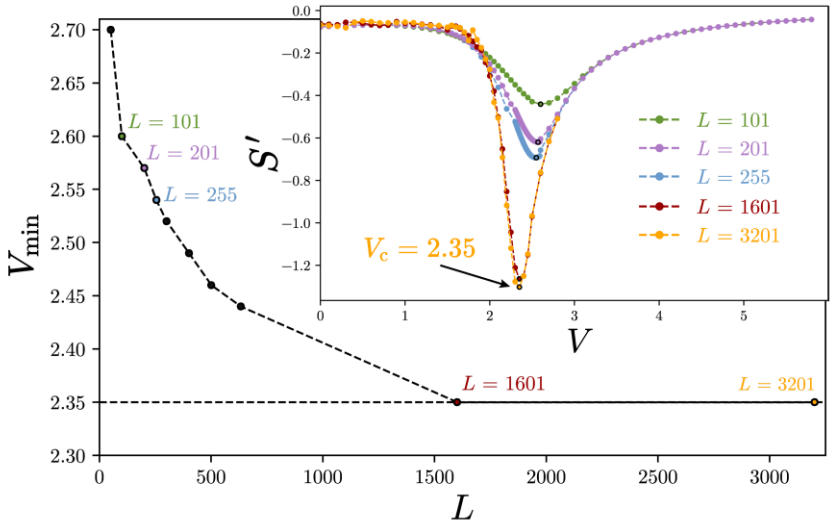

Figure 2.3: Minimum V_{min} of the slope $S'(V)$ of entropy approaches the region of the numerical critical value $V_c = 2.35$. An odd chain with CCS is used.

Parity [CCS]	V_c	Deviation
Even [both]	2.15	7.5%
Odd [yes]	2.35	17.5%
Odd [no]	2.5	25%

Table 2.1: Critical values using minima of $S'(V)$ and their maximum deviation from the theoretical value. Even chain has two local minima. Here, the minimum closer to the critical point was taken.

A better way to determine the critical value is to use the **P**hase **I**ndependent **F**it method described in Chapter 1.7.4, as shown in Figure 2.4.

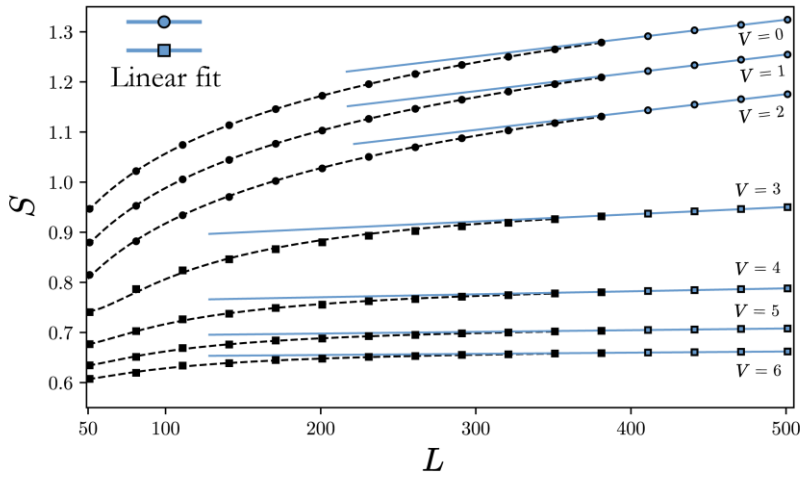

Figure 2.4: Phase-independent linear fit of the entropy $S(L)$ for different V. Only the colored four points representing large L are fitted.

For lengths starting at approximately $L \approx 400$, the entropy $S(L)$ is phase-independently linear. Therefore, a linear fit is suitable here:

$$S(V, L > 400) = S'V + a \tag{2.2}$$

The determined **slopes** $S'(V)$ are plotted for different interaction potentials V. In the vicinity of the critical region, there is a maximum $S'(V_c)$ at V_c deviating 10% to 20% from the exact value $V_{cdw} = 2$ (see Table 2.2).

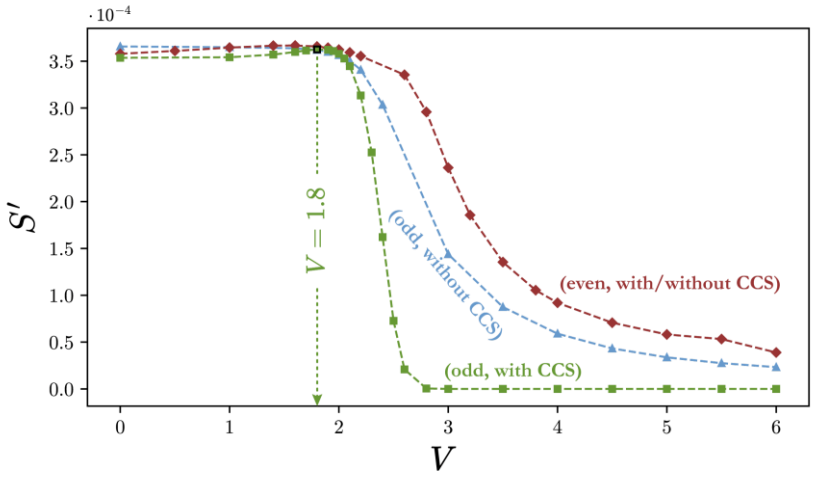

Figure 2.5: Slopes $S'(V)$ from the linear fits of $S(L)$ for different V and other parameters of the chain. A maximum occurs near the phase transition.

Parity [CCS]	V_c	Deviation
Even [both]	1.6	20%
Odd [yes]	1.8	10%
Odd [no]	–	–

Table 2.2: Determined critical values using the linear fit of entropy $S(L)$. Odd chain without CCS has no local extremum.

There is a possibility to bring the critical value still far below 10% deviation. For this purpose, the $S(L)$ curves for different L starting at length $L \approx 200$ are fitted with the power law (1.24) (**P**hase **I**ndependent **F**it method), as shown in Figure 2.7. The extracted **exponents** $\kappa(V)$ are plotted as a function of V and the **maximum** V_c is read off from the plot.

As Figure 2.6 shows, the critical value can be determined surprisingly well with the **P**hase **I**ndependent **F**it method - the deviation from the exact value is less than 5% for an *odd* chain *with/without* CCS!

The **error** V_{err} of the critical value $V_c \pm V_{err}$ is determined by the distance of V_c to the neighboring point V and it is assumed to be the most dominant error in this work.

Parity [CCS]	$V_c \pm V_{err}$	Deviation
Even [both]	2.1 ± 0.05	7.5%

Parity [CCS]	$V_c \pm V_{err}$	Deviation
Odd [both]	2 ± 0.05	2.5%

Table 2.3: Determined critical values by using the power law fit of entropy $S(L)$.

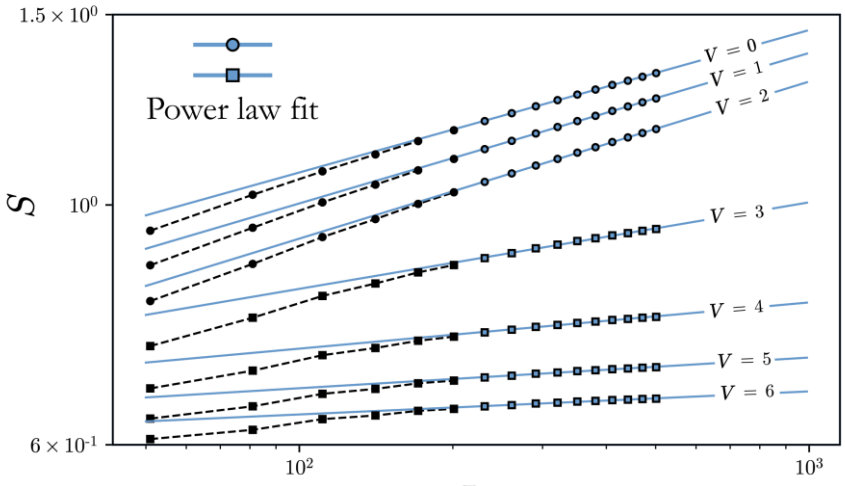

Figure 2.7: Finite-size scaling $S(L)$ of entropy on a double logarithmic scale. The blue points are fitted with the power law. Dashed lines are for eye guidance.

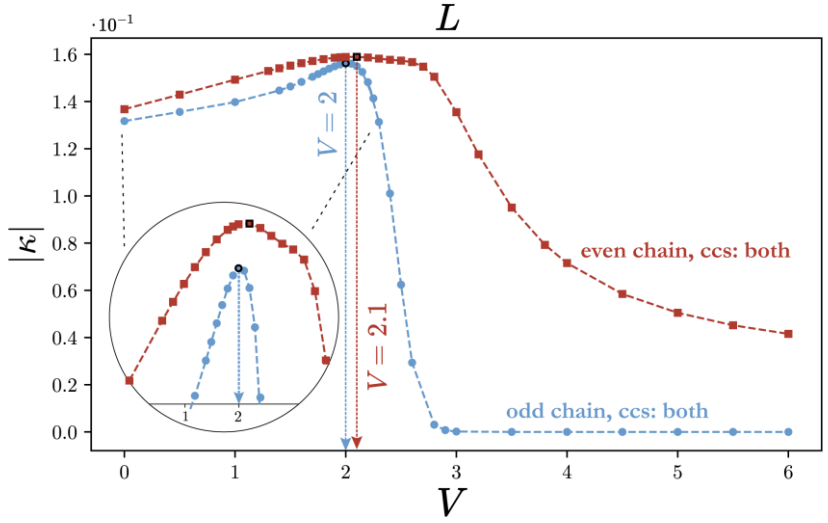

Figure 2.6: Exponents extracted from the fit of $S(L)$ for different V. Dashed lines are for eye guidance.

2.2. CENTRAL CHARGE

In order to determine **central charge** $c(V)$, the entropy must be determined for two *different* lengths L and L'. Figure 2.9 and Figure 2.8 show central charge $c(V)$ as a function of V for different **length combinations** (L, L'). Figure 2.9 shows simulations *without* and Figure 2.8 *with* CCS. The combinations without CCS are less accurate in determining the critical value and deviate more from the behavior in the thermodynamic limit as described in Chapter 1.6.2. Therefore, the simulations without CCS are not discussed further here.

- $(L, L') = (\mathbf{odd}, \mathbf{odd})$: This combination *with* CCS is length independent and best reflects the predictions of the theory, namely $c(V) = 1$ for small V and $c(V) = 0$

for large V. Near the theoretically predicted phase transition at $V_{cdw} = 2$, a **maximum** V_c occurs.

- $(L, L') = (\mathbf{odd}, \mathbf{even})$: This combination *with* CCS has a neither perfectly formed metallic phase nor a CDW phase. Near the theoretical phase transition, $c(V)$ falls into the negative because here the shorter even chain is more entangled than the longer odd chain: $S(L') > S(L)$.[4] The $c(V)$ curve has a maximum, which, however, would provide a less accurate critical value than for the $(\mathrm{odd}, \mathrm{odd})$ length combination. What is interesting about this length combination is the **zero crossing** $c(V_c) \approx 0$, which happens near the critical point and becomes more accurate with a smaller length difference $L' - L$. Whether this zero crossing is purely "accidental" near $V_{cdw} = 2$ is unclear. The disadvantage of this zero crossing is that it is length dependent. A *length-independent* candidate for the critical point V_c is the *intersection* of all $c(V)$ curves of different length combinations.
- $(L, L') = (\mathbf{even}, \mathbf{even})$: In this combination, the CDW phase is hardly formed and is only reached for very large $V \geq 6$. Also the maximum has a deviation of more than 30% from the critical value.
- $(L, L') = (\mathbf{even}, \mathbf{odd})$: With this combination, the metallic phase is maintained to approximately $V \approx 2$, as predicted by theory. Starting from $V \approx 2$, however, it does not fall to zero, but increases and saturates at a positive finite value. This combination, unlike all other length combinations, yields a minimum in the phase transition region.

The $(\mathbf{even}, \mathbf{odd})$ as well as $(\mathbf{even}, \mathbf{even})$ length combination with CCS, but also all length combinations without CCS seem to be rather useless for the determination of the critical point. The combinations $(\mathbf{odd}, \mathbf{odd})$ and $(\mathbf{odd}, \mathbf{even})$ on the other hand provide useful possibilities to determine the critical point approximately. Therefore, these length combinations will be applied to the (alternating) ladder in the next chapters. Table 2.4 summarizes the results with CCS to determine the critical point using central charge.

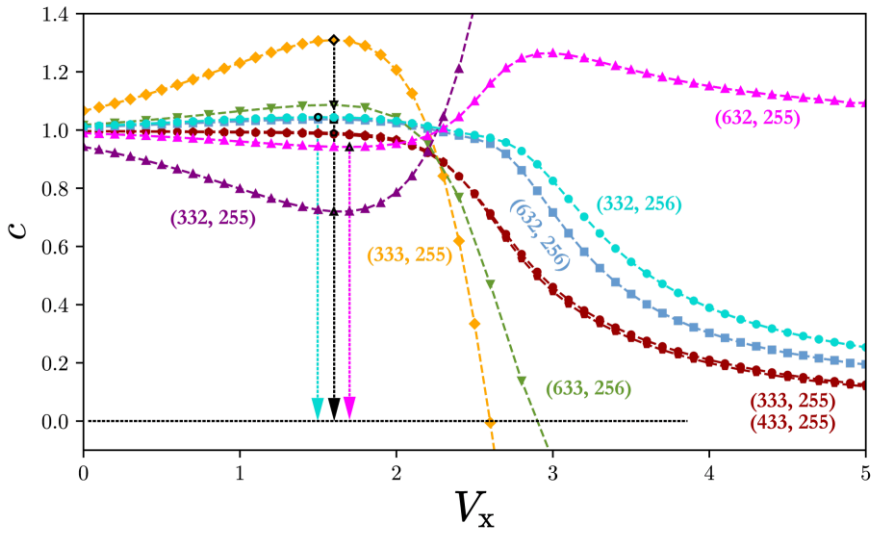

Figure 2.9: Central charge as a function of V **without CCS** for different length combinations.

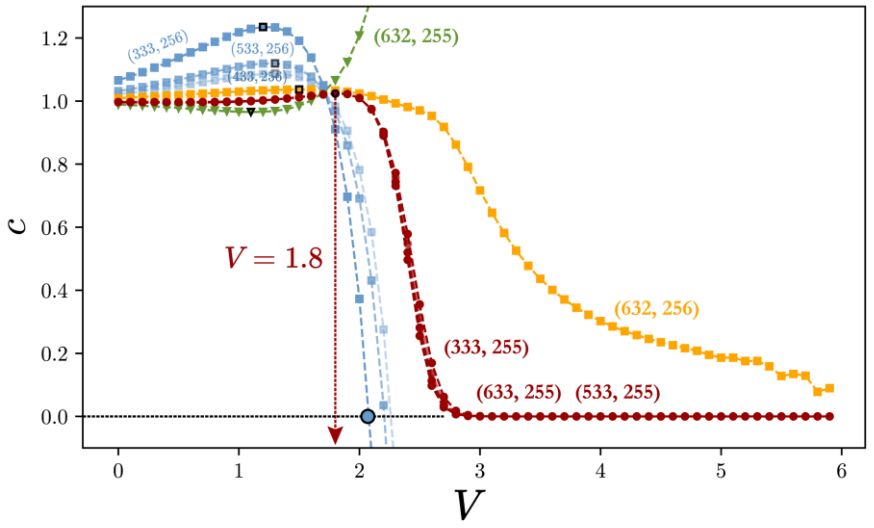

Figure 2.8: Central charge as a function of V **with CCS** for different length combinations.

Method	(L, L')	CCS	V_c	Deviation
Extremum in $c(V)$ of a **F**inite **S**ystem	$(333, 255)$	yes	1.85 ± 0.01	13%
Zero **C**rossing $c(V_c) = 0.001 \approx 0$	$(333, 256)$	yes	2.08 ± 0.01	4%

Table 2.4: Determined critical value V_c and its deviation from the theoretical value by using central charge.

2.3. EXCITATION GAP

Figure 2.10 shows the **energy gap** $\Delta E(V)$ as a function of V for an *odd* chain length *without* CCS. As can be seen, the energy gap decreases with larger L for all V. This behavior is also observed for an *even* chain *with/without* CCS. To verify the implementation of the program, the exact energy (1.7) of a non-interacting chain is compared with the calculated values $\Delta E(V = 0)$. They agree perfectly.

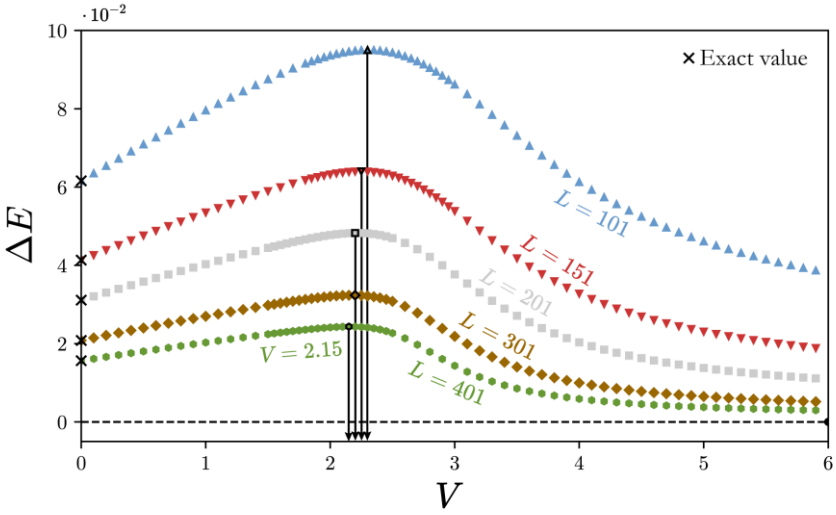

Figure 2.10: Energy gap as a function of V has a maximum that shifts with increasing length to the phase transition $V_{\text{cdw}} = 2$.

As Figure 2.11 shows, the energy gap $\Delta E(V)$ vanishes (to within two decimal places) in the thermodynamic limit in both phases. This behavior is theoretically expected, as described in the introductory chapter: In the metallic phase $(V \leq 2)$ no energy gap exists and in the CDW phase $(V > 2)$ the ground state is doubly degenerate, which is why the difference of the smallest two energy eigenvalues of the Hamiltonian (1.8) or (1.9) is zero. The finite-size effects as well as DMRG truncation lead to the fact that the energy gap $\Delta E(V)$ is not perfectly zero.

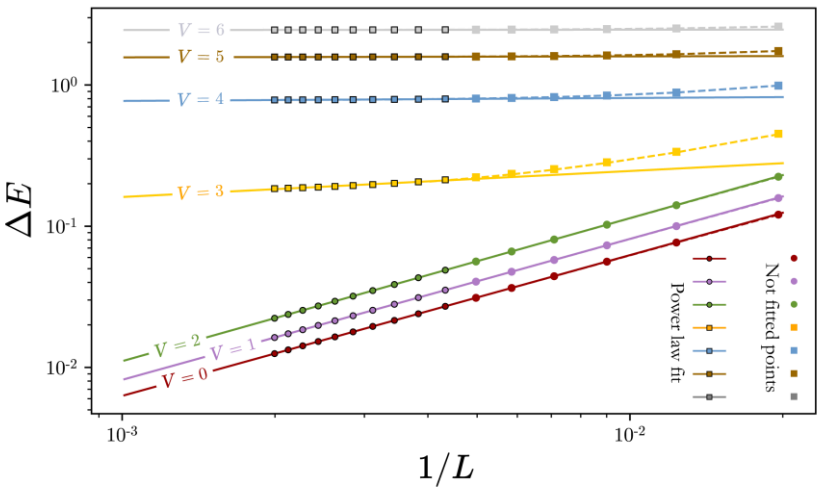

Figure 2.11: On a double logarithmic plot, the energy gap $\Delta E(1/L)$ is linear in the metallic phase for all L and linear only for large L in the CDW phase. The bordered points are fitted with the power law. The dashed lines are for eye guidance.

Figure 2.11 also reveals that the energy gap falls off *at different rates* in the two phases:

- **For V smaller than 2**: For *odd*/*even* chain lengths *with*/*without* CCS, the energy gap $\Delta E(1/L)$ as a function of $1/L$ shows linear behavior for all L. Thus, the energy gap $\Delta E(1/L)$ obeys a *power law*. In this phase, the power law exponent is $\kappa = 1$.
- **For V larger than 2**: There is a deviation of $\Delta E(1/L)$ from a linear behavior on a double-logarithmic scale for small L. In this phase, the power law exponent is $\kappa = 0$ for larger L starting at $L \approx 100$. The different value of the exponent in different phases is later exploited to determine the critical value.

The $\Delta E(V)$ data points for *finite* chain lengths also show a **length-dependent maximum** that shifts toward the theoretically predicted phase transition with increasing length (see Figure 2.10).

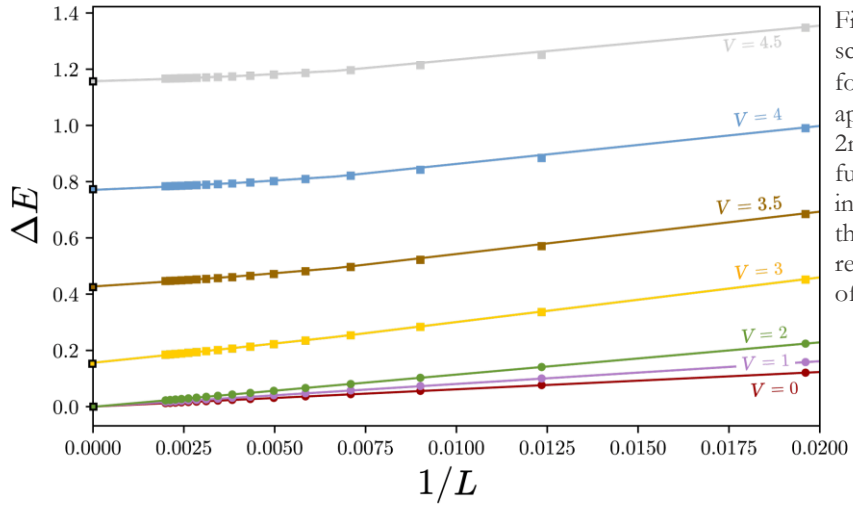

Figure 2.12: Finite-size scaling of the energy gap for different V, approximated by the 2nd order polynomial function. The intersection points with the vertical axis represent the energy gap of an infinite chain.

How does $\Delta E(1/L)$ behave as a function of $1/L$ for an *odd* chain *with* CCS? Here it also approaches zero in the metallic phase with the power law, but in the CDW phase the energy gap approaches a **non-zero value** ΔE_∞ polynomially of second order[3] (Figure 2.12):

$$\Delta E\left(\frac{1}{L}\right) = A\left(\frac{1}{L}\right)^2 + B\frac{1}{L} + \Delta E_\infty \tag{2.3}$$

Why this different behavior? For *even* chains the CDW ground state is degenerate, therefore $\Delta E(1/L)$ goes to zero in the thermodynamic limit. For *odd* chains *with* CCS, on the other hand, the degeneracy is lifted because the two degenerate states $|E_0\rangle$ and $|E_1\rangle$ have different particle numbers: $N_0 = (L+1)/2$ and $N_1 = N_0 - 1$ (see Figure 1.6). Thus, at first glance, ΔE should correspond to the single-particle gap E_p discussed in Chapter 2.4. However, the simulation of the excitation gap (Figure 2.13) yields only *half* of the

single-particle gap (Figure 2.15). The reason for this is the rounding off of the number of particles N in the case of odd chains, which leads to a chain that is *not half-filled*. For example, for a chain with $L = 5$, the fermion number $N = L/2$ is rounded off to 2.

The extraction of the intercepts $\Delta E_\infty(V)$ for different V of and odd chain with CCS yields the behavior of $\Delta E(V)$ in the thermodynamic limit (see Figure 2.13):

- **For V much smaller than 2**: The energy gap $\Delta E(V)$ is zero.
- **Near the phase transition** ($V \approx 2$): The energy gap $\Delta E(V)$ opens exponentially according to Eq. (1.23).
- **For V much larger than 2**: The energy gap $\Delta E(V)$ is proportional to V.

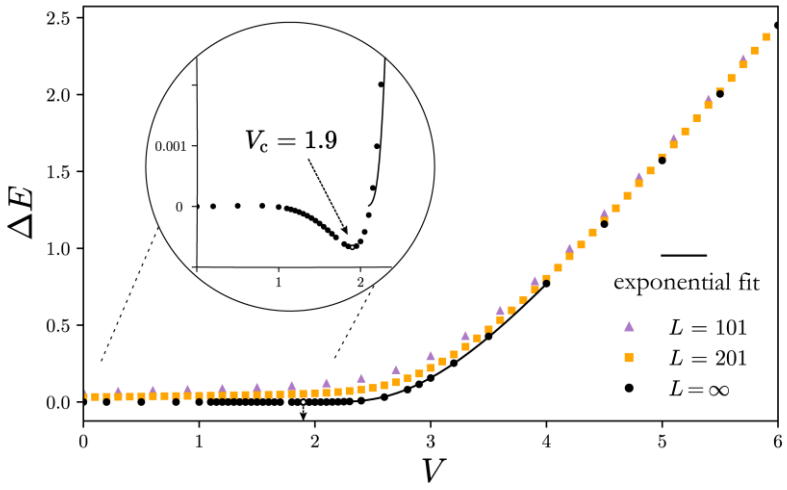

Figure 2.13: Excitation gap $\Delta E(V)$ of an odd chain length with CCS exhibits a minimum and behaves exponentially near the phase transition.

The exponential behavior at the phase transition allows the extraction of the critical value with the **E**xponential **F**it **N**ear **O**pening **G**ap method, by fitting the energy gap $\Delta E(V)$ in the range: $2.1 < V < 6$ using Eq. (1.23). The resulting critical value of $V_c = 2.01 \pm 0.06$ is very close to the theoretical value $V_{cdw} = 2$, but there is a deviation in V_c depending on whether the arbitrary upper fit limit is chosen at $\overline{V} = 4$ or, for example, at $\overline{V} = 6$. The resulting (estimated) error is $V_{err} \approx 0.06$. As mentioned in the introductory chapter, for the **E**xponential **F**it **N**ear **O**pening **G**ap method, the observables are always fitted between $\underline{V} = 2.1$ and $\overline{V} = 6$.

The observed power law behavior (Figure 2.11) in finite-size scaling of $\Delta E(1/L)$ in both phases, allows the **P**hase **I**ndependent **F**it with the power law (1.24). Figure 2.14 shows the **exponents** $|\kappa(V)|$ extracted from the fits in Figure 2.11. As can be seen, the exponent $|\kappa(V \ll 2)| = 1$ as a function of V is constant 1 in the metallic phase, bends to an extremum at the phase transition and saturates in the CDW phase either at $|\kappa(V \gg 2)| =$

2 or at $|\kappa(V \gg 2)| = 0$. The extremum of $|\kappa(V)|$, for example for an *odd* chain *with* CCS, has **only a deviation of 2.5%** from the theoretical value $V_{\mathrm{cdw}} = 2$ in the thermodynamic limit!

The following Table 2.5 summarizes all methods that, applied to the excitation gap, approximate a theoretical critical value $V_{\mathrm{cdw}} = 2$. The rows marked in green represent the best methods with accuracy below 5%.

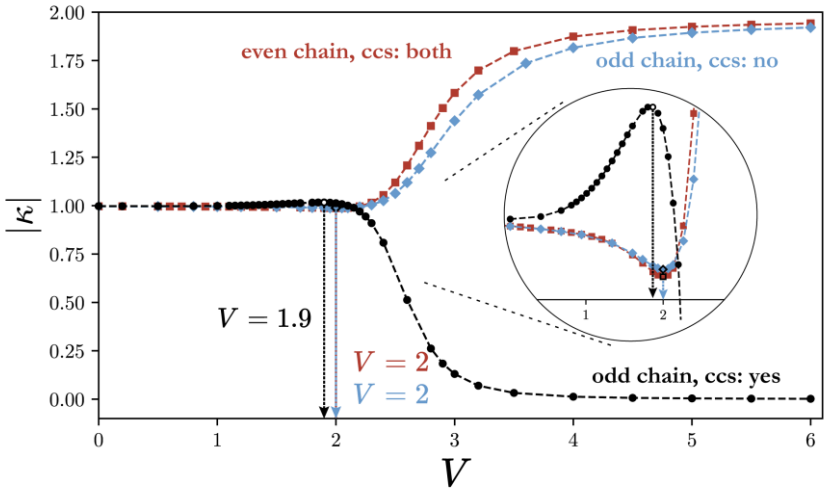

Figure 2.14: Exponents $|\kappa(V)|$ extracted from the fits for different V. They exhibit an extremum at the phase transition.

Method	Parity [CCS]	$V_c \pm V_{\mathrm{err}}$	Deviation
Extremum in $\Delta E(V)$ of an **I**nfinite **S**ystem	Odd [yes]	1.9 ± 0.05	7.5%
Exponential **F**it near the **O**pening **G**ap	Odd [yes]	2.01 ± 0.06	3.5%
Extremum in $\Delta E(V)$ of a **F**inite **S**ystem	Odd [no]	2.10 ± 0.05	7.5%
Extremum in $\Delta E(V)$ of a **F**inite **S**ystem	Even [both]	2.05 ± 0.05	5%
Phase **I**ndependent **F**it of $\Delta E(1/L)$	Even [both]	2 ± 0.05	2.5%
Phase **I**ndependent **F**it of $\Delta E(1/L)$	Odd [yes]	1.9 ± 0.05	7.5%
Phase **I**ndependent **F**it of $\Delta E(1/L)$	Odd [no]	2 ± 0.05	2.5%

Table 2.5: Extracted critical values V_c with different methods applied to the calculated energy gap $\Delta E(V)$.

2.4. SINGLE-PARTICLE GAP

Theoretically, the **single-particle gap** $E_p(V)$ for an infinite chain opens exponentially at the transition $V_{cdw} = 2$ to the CDW phase according to Eq. (1.23) and increases linearly with V in the CDW phase. This behavior is confirmed for finite *even* chains *with/without* CCS and for *odd* chains *with* CCS in the extrapolated thermodynamic limit.

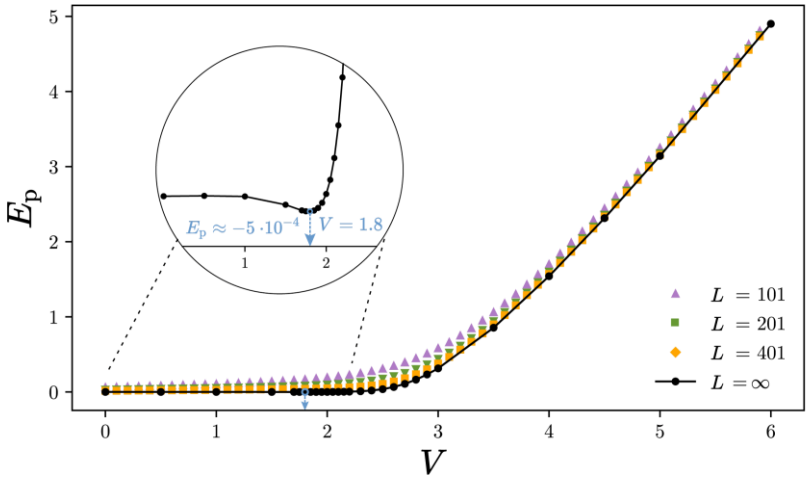

Figure 2.15: Single-particle gap $E_p(V)$ for odd lengths with CCS. The extrapolated curve for an infinite chain shows a minimum near the phase transition.

Figure 2.15 shows single-particle gap $E_p(V)$ as a function of V for different *odd* chain lengths *with* CCS. To obtain the $E_p(V, L \to \infty)$ curve for an infinite chain, the data points $E_p(1/L)$ as a function of $1/L$ are fitted with a polynomial function of second order (2.3) as in the case of the energy gap investigated in the previous chapter and extrapolated up to the vertical intercept. Zooming in close to the phase transition reveals a **minimum** at $V_c = 1.8 \pm 0.05$, which deviates from the theoretical value by 12.5%. However, this minimum is very small, so it is probably sensitive to convergence errors.

Of course, the exponential opening of the gap above the phase transition $2.1 \leq V \leq 6$ can also be fitted with Eq. (1.23) to determine the critical value. In this case, the result is a more accurate value $V_c = 1.92 \pm 0.09$ which differs from the theoretical value by 8.5%.

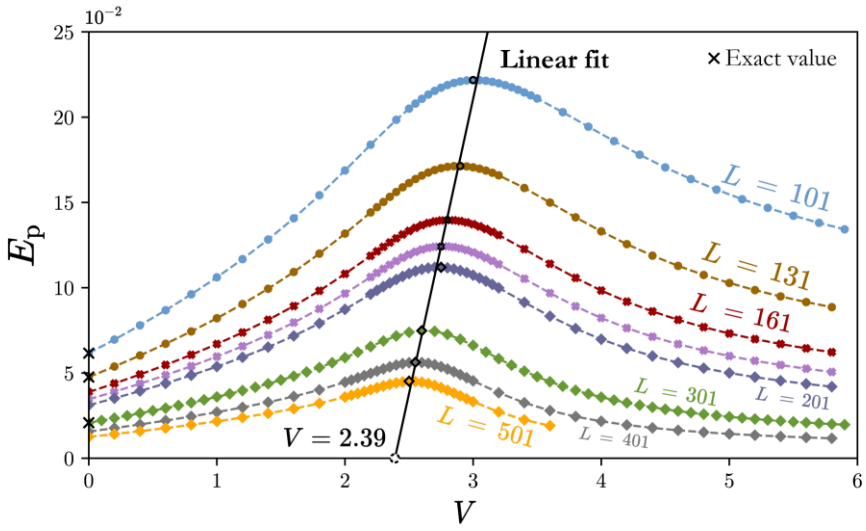

Figure 2.16: Single-particle gap for an odd chain without CCS decays to zero in the CDW phase and has a length-dependent maximum.

A completely different behavior is shown by the single-particle gap $E_p(V)$ as a function of V for an *odd* chain length *without* CCS (see Figure 2.16):

- **For $V \lesssim 2$**: Single-particle gap $E_p(V)$ decreases with the power law (1.24) with increasing length.
- **Near the phase transition ($V \approx 2$)**: Single-particle gap $E_p(V)$ grows and reaches a maxmum V_{max} and then decreases with V. The maxmum is length dependent and shifts in the direction of the theoretical phase transition of an infinite chain, but does not reach the correct value $V_{cdw} = 2$.
- **For $V \gtrsim 2$**: Single-particle gap $E_p(V)$ decreases for large lengths with the power law. For the parameter choice (odd, *without* CCS), the single particle gap $E_p(V)$ behaves like the previously discussed energy gap ΔE of an even chain *with*/*without* CCS or odd chain *without* CCS.

All $E_p(V)$ data points have an extremum, so methods from Chapter 1.7.1 (for a finite system) or from Chapter 1.7.2 (for an extrapolated infinite system) can be used to determine the critical point (see Table 2.6):

- **E**xtremum in $E_p(V)$ of a **F**inite **S**ystem method is applied to the *odd* chain *without* CCS and requires in this case the correct choice of a fit function for the maxima

shift. A linear fit seems to be unsuitable here, which is why this method yields a deviation of 20% from the theoretical value.

- **E**xtremum in $E_p(V)$ of an **I**nfinite **S**ystem method is applied to chains with all other parameters. It is applied to the minimum of $E_p(V)$ for an infinite chain extrapolated from finite-site scaling. The minimum has a deviation of 10% from the theoretical value. The inaccuracy could be due to the fact that the minimum is small: $E_p(V_c) \approx 10^{-4}$ and starting at the fourth decimal place the convergence error distorts the result.

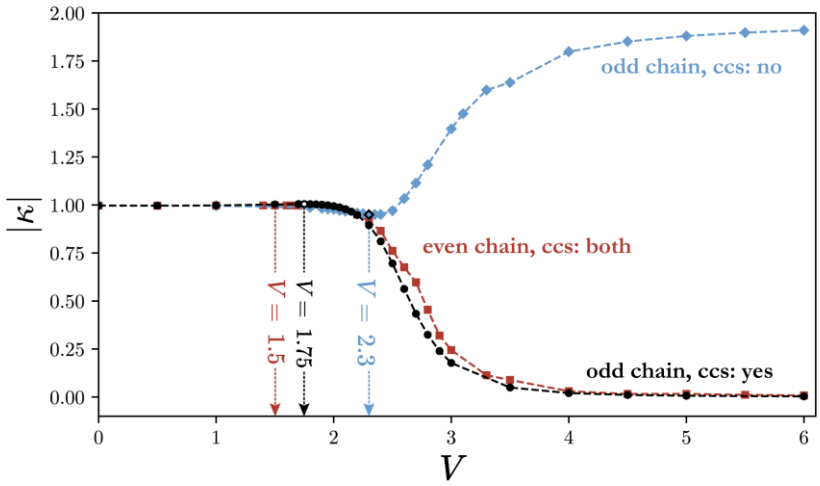

Figure 2.17: The extracted exponents $|\kappa|(V)$ of the powerlaw fit as a function of V are 1 in the metallic phase and saturate in the CDW phase. There is an extremum close to the phase transition.

The application of the **P**hase **I**ndependent **F**it method to the finite-size scaling of $E_p(1/L)$ also does not give a more accurate result for the critical value, as Table 2.6 shows. However, the behavior of the exponent $|\kappa(V)|$ as a function of V is interesting (see Figure 2.17):

- **The exponent $|\kappa|$ approaches $|\kappa| \to 2$** for $V \to \infty$ if the single-particle gap E_p or the excitation gap ΔE do not open in the CDW phase.
- **The exponent $|\kappa|$ approaches $|\kappa| \to 0$** for $V \to \infty$ if the single-particle gap E_p or the excitation gap ΔE open exponentially, as theoretically predicted, and increase linearly for large V. In this case, the exponent $|\kappa(V)|$ behaves similarly to the previously discussed central charge $c(V)$ as a function of V for (odd, odd)-length combinations. In a future work, it would be interesting to investigate how the quantities $c(V)$ and $|\kappa(V)|$ are theoretically related.

Table 2.6 summarizes all methods applied to the single-particle gap. The methods marked in green are best suited for this observable.

Method	Parity [CCS]	V_c	Deviation
Extremum in $E_p(V)$ of an **I**nfinite **S**ystem	Even [both]	1.8 ± 0.1	10%
Extremum in $E_p(V)$ of an **I**nfinite **S**ystem	Odd [yes]	1.8 ± 0.05	10%
Extremum in $E_p(V)$ of a **F**inite **S**ystem	Odd [no]	2.39 ± 0.05	19.5%
Exponential **F**it **N**ear **O**pening **G**ap	Even [both]	1.945	2.75%
Exponential **F**it **N**ear **O**pening **G**ap	Odd [yes]	1.928 ± 0.01	3.65%
Phase **I**ndependent **F**it of $E_p(1/L)$	Odd [no]	2.3 ± 0.05	17.5%
Phase **I**ndependent **F**it of $E_p(1/L)$	Odd [yes]	1.75 ± 0.1	17.5%
Phase **I**ndependent **F**it of $E_p(1/L)$	Even [both]	1.5 ± 0.1	30%

Table 2.6: Extracted critical values V_c with different methods applied to the calculated single-particle gap $E_p(V)$. If no error V_{err} is specified, then it is negligible.

2.5. CDW ORDER PARAMETER

The **CDW order parameter** $\delta(V)$ theoretically reveals the phase transition in the thermodynamic limit, increasing from $\delta(V) = 0$ in the metallic phase to the value $\delta(V) = 0.5$ for $V \to \infty$.[3] Simulation of the magnitude $|\delta(V)|$ on a *finite* chain shows similar behavior. However, convergence with L is not sufficient to efficiently and accurately extract the theoretical critical value $V_{cdw} = 2$.

- **Odd chain with CCS**: In the region $V \lesssim 2$, the order parameter $|\delta(V)|$ approaches zero with increasing chain length L. No extremum occurs in the critical region, as in the case of the single-particle gap $E_p(V)$ and excitation gap $\Delta E(V)$. In the region $V \gtrsim 3$, the order parameter is length-independent and, as theoretically expected, approaches $|\delta(V)| = 0.5$ for $V \to \infty$ (see Figure 2.18). The convergence of the order parameter $|\delta(V)|$ can be fitted with the 2nd degree polynomial (1.18). The obtained limit value differs only by 0.00004% from the theoretical limit $|\delta(V \to \infty)| = 0.5$.

To obtain the order parameter $|\delta(V, L \to \infty)|$ for an *infinite* chain, the data points $|\delta(L)|$ for different V are extrapolated with a polynomial function of second order (2.3), in the same way as for the single-particle gap and excitation gap. However, for the order parameter the polynomial fit does not work so well, as Figure 2.18 shows. In the region $V \lesssim 2$ the order parameter $|\delta(V)|$ for length $L = 2401$ converges to zero better than the polynomially extrapolated thermodynamic limit.

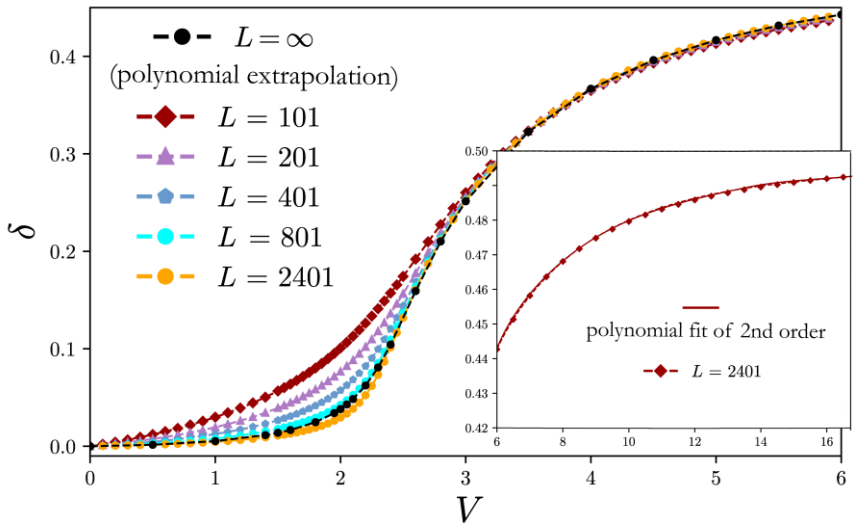

Figure 2.18: Magnitude $|\delta(V)|$ of the order parameter for odd lengths with CCS converge very slowly to the thermodynamic limit. The inset shows the behavior of the order parameter for large V.

- **Even chain with/without CCS and odd chain without CCS**: Here, the behavior in the metallic phase is the same as for an odd chain with CCS. The order parameter $|\delta(V)|$ for larger V on the other hand, remains much smaller than 0.5. This is because DMRG here leads to a *linear combination* of the two ground states $|E_0\rangle$ and $|E_1\rangle$ (see Figure 1.10).

For such an observable as $\delta(V)$, which has neither an extremum nor a discontinuity, the **derivative** $|\delta'(V)| = |\Delta\delta|/\Delta V$ can be investigated to see if it has an extremum. As Figure 2.19 shows, the derivative indeed shows a maximum, which moves into the theoretically predicted critical region for longer chains. However, the convergence is poor here and the limit $L \to \infty$ does not lead the maximum to the position $V_{\mathrm{cdw}} = 2$. Table 2.7 summarizes the determined maxima using the derivative of the CDW order parameter.

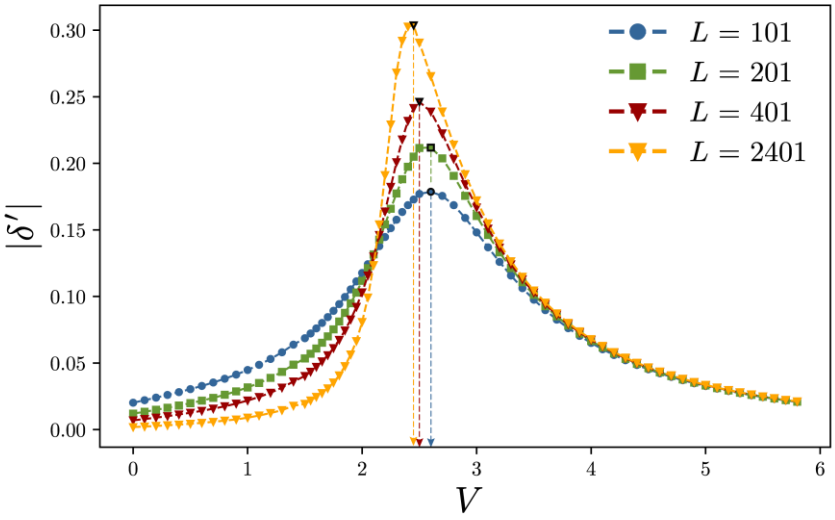

Figure 2.19: Derivative $|\delta'(V)|$ of the order parameter for an odd chain with CCS exhibits a length-dependent maximum.

Method	Parity [CCS]	V_c	Deviation
Extremum in $\|\delta'(V)\|$ of a **F**inite **S**ystem for $L = 801$	Odd [no]	2.6 ± 0.1	35%
Extremum in $\|\delta'(V)\|$ of a **F**inite **S**ystem for $L = 2401$	Odd [yes]	2.45 ± 0.05	25%
Extremum in $\|\delta'(V)\|$ of a **F**inite **S**ystem for $L = 400$	Even [both]	2.6 ± 0.1	35%

Table 2.7: Critical values V_c and their maximum deviation from the theoretical value $V_{cdw} = 2$ by using the maximum of the magnitude $|\delta'(V)|$ of the derivative of the CDW order parameter.

The application of other methods to extract the critical value do not work here. The **P**hase **I**ndependent **F**it method in combination with the power law *can be applied* here, but the resulting exponent $|\kappa(V)|$ as a function of V does not have an extremum.

2.6. Density fluctuation

Just like the CDW order parameter, the **density fluctuation** σ^2 exploits the particle densities $\langle n_x \rangle$. However, the density fluctuation $\sigma^2(V)$ as a function of V shows a more pronounced transition from the metallic to the insulating phase, as exemplified by Figure 2.20 for an *odd* chain *with* CCS. The interpretation of the results is analogous to the interpretation of the results of the CDW order parameter:

- **Odd chain with CCS**: In the region $V \lesssim 2$, the density fluctuation $\sigma^2(V)$ approaches zero with increasing chain length L. Density fluctuation near the phase transition $V \approx 2$ does not show an extremum. In the region $V \gtrsim 3$, the density fluctuation is length independent and approaches $\sigma^2(V) \to 0.25$ for $V \to \infty$ as theoretically expected. The fit of the finite-size scaling $\sigma^2(1/L)$ with a polynomial function of second order provides a better extrapolation of the thermodynamic limit than the CDW order prameter, as can be seen in Figure 2.18.
- **Even chain with/without CCS** and **odd chain without CCS**: Here, the behavior in the region $V \lesssim 2$ is the same as for an *odd* chain *with* CCS. In contrast, the density fluctuation $\sigma^2(V)$ remains small: $\sigma^2 \ll 0.25$, even for large V. The reason here is the same as for the CDW order parameter: The linear combination of the two degenerate ground states $|E_0\rangle$ and $|E_1\rangle$ hides the inhomogeneous density of the CDW phase.

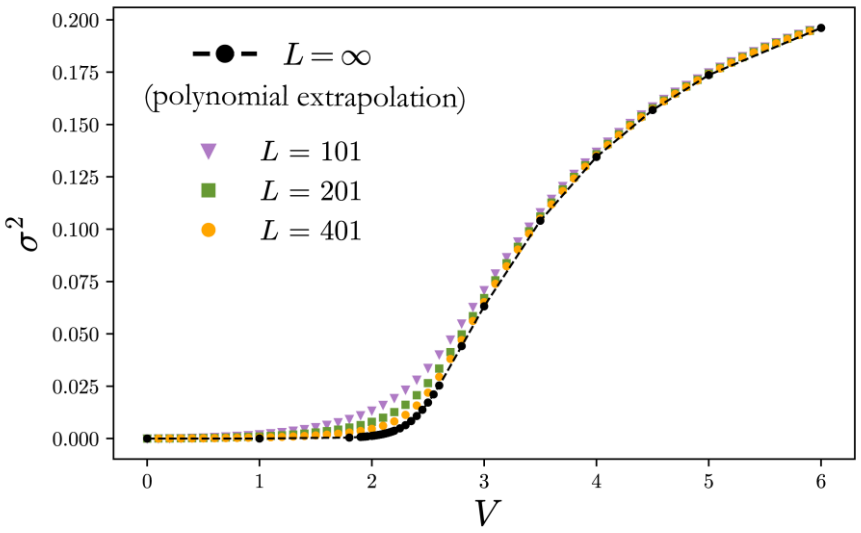

Figure 2.20: Density fluctuation $\sigma^2(V)$ for an odd chain with CCS converges better to zero for $V \lesssim 2$ than CDW order parameter.

The **derivative** $\sigma^2(V)'$ as a function of V has a **maximum** like the CDW order parameter. The deviation of the position V_{max} of the maximum can be reduced by increasing the chain length, but the convergence $L \to \infty$ is worse than for the CDW order parameter. Therefore, the determined critical values V_c are not presented here.

2.7. DENSITY-DENSITY CORRELATION FUNCTION

The **magnitude** $|F(x)|$ of the **density-density correlation function** is shown in Figure 2.21 as a function of the **distance** x to the **fixed point** $x_0 = L/2$ on a double logarithmic scale for an *odd* length $L = 401$ *with/without* CCS.

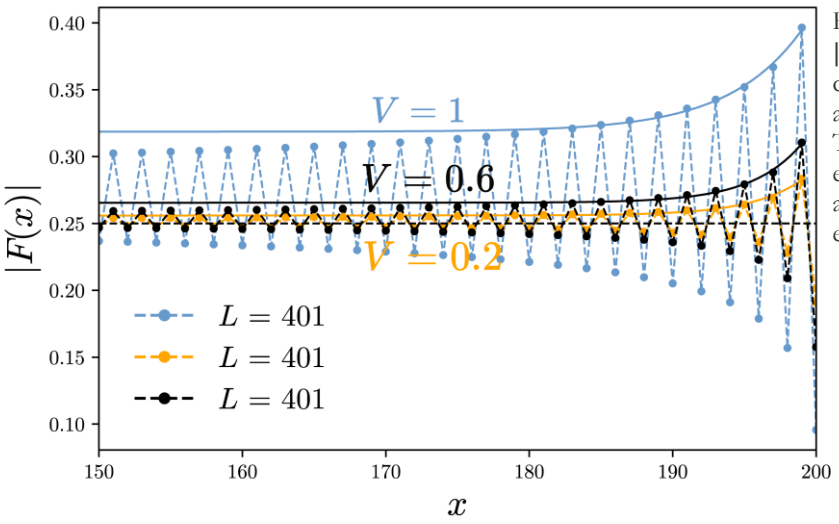

Figure 2.21: Magnitude $|F(x)|$ of the correlation function for an odd chain with CCS. The amplitude at the edge increases approximately exponentially.

The correlation function oscillates around the value $|F(x)| \approx 0.25$, and the amplitude increases close to the chain edge (a boundary effect known as Friedel oscillation)[15]. The amplitude of the oscillation increases with larger interaction potential V for all x. The same behavior is observed for an *even* length *with/without* CCS. The only difference is that the oscillation for a fixed V is smaller than for odd chain lengths. No power law (1.21) is observed as described in Chapter 1.6.8. Thus, method #5 cannot be used to extract the Luttinger Liquid parameter to determine the critical value. Interestingly, power law can be observed when the right block in the DMRG algorithm is taken as a **reflection of the left block** (of course, this reflection symmetry only works for even chains). Then the correlation function $F(x - x_0)$ shows oscillations and decays for a not too large distance $|x - x_0|$ according to the power law (1.21). Figure 2.22 shows the difference of an even chain with and without reflection symmetry.

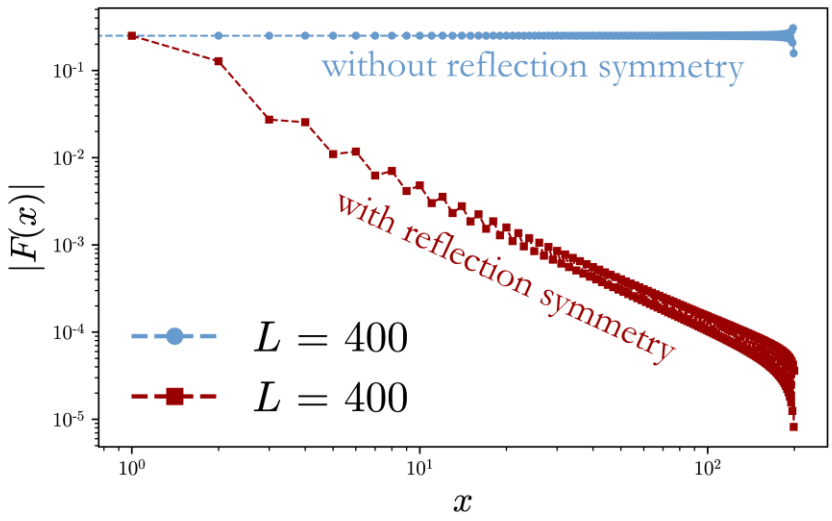

Figure 2.22: Comparison of the correlation function for an even chain with/without reflection symmetry and $x_0 = 1$. A chain with reflection symmetry falls off with the power law.

Consequently, from the exponent of the power law fit, the **LL parameter** $K(V)$ can be extracted as a function of V. For $K(V_c) = 0.5$ it should mark the breakdown of the **L**uttinger **L**iquid - thus providing the critical value V_c. However, the oscillations of $|F(x)|$ and no-power-law behavior for large x, make it difficult to extract the LL parameter. This is because a blunt fit of all data points $|F(x)|$ gives a useless result. Therefore, only the medium distances for different V are fitted, as shown in Figure 2.23.

The extracted LL parameter $K(V)$ from the power law (1.21) is plotted as a function of

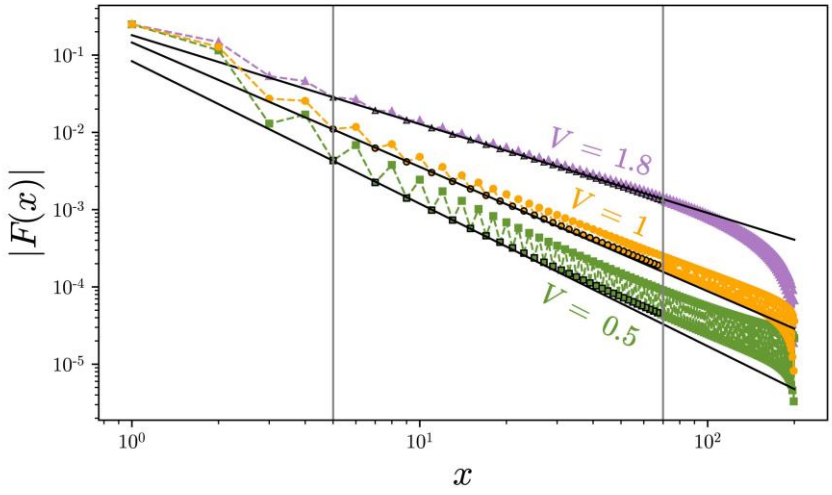

Figure 2.23: Magnitude $|F(x)|$ of the correlation function for an even chain with/without CCS. Only the black points are fitted with the power law for different V. The fitted region is outlined with the two vertical lines.

V and compared with the theoretical curve (1.22) in the thermodynamic limit in Figure 2.24. As can be seen, the calculated curves $K(V)$ for $L = 400$ and even for $L = 1000$ deviate from the result of an infinite chain in the range $0 < V < 1.5$. However, the deviation decreases with the length. In the range $1.5 < V < 2$ the agreement with the

infinite chain is better. Therefore, the critical value can be read off at the point $K(V_c) \approx 0.5$. The extracted critical points are summarized in Table 2.8.

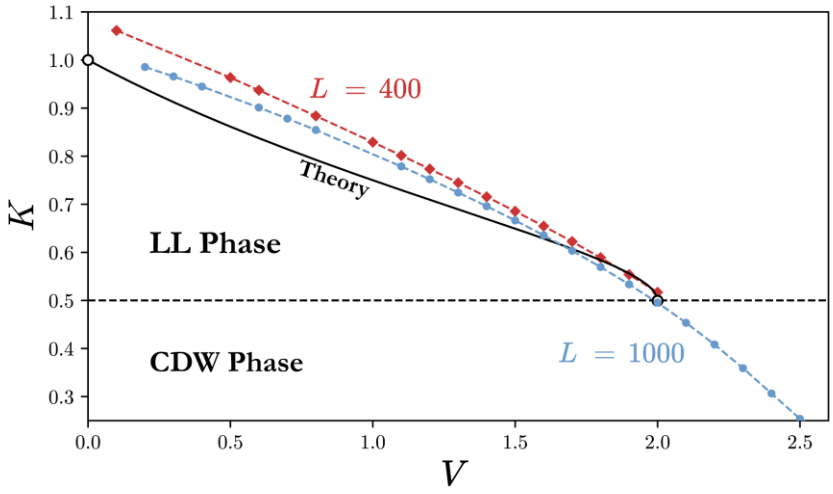

Figure 2.24: The LL parameters $K(V)$ extracted from the powerlaw fit of the correlation functions deviate from the theoretical curve for an infinite chain. However, the $K(V)$ still provides a good estimate of the critical point.

The application of the following correction terms[1] gives no improvement in the determination of the LL parameter by means of the correlation function:

$$F(x) = \frac{C_1}{x^2} + C_2(-1)^x + \left(\frac{1}{x}\right)^{2K}, \quad \text{for } V < 2 \tag{2.4}$$

Method	Parity [CCS]	V_c
Intercept of $K = 0.5$ for $L = 400$	Even [yes]	~ 2.01
Intercept of $K = 0.5$ for $L = 1000$	Even [yes]	~ 2.0

Table 2.8: Intersection point $K(V_c)$ of the curve $K(V)$ with the horizontal line through the point $K = 0.5$ provides the critical value V_c.

2.8. SUMMARY

For most observables investigated, the calculated results of a *finite* 1DSF chain with *odd* length and *with* CCS agree well with the theory's predictions in the thermodynamic limit. To determine the theoretical phase transition $V_{cdw} = 2$ of a 1DSF chain, **four observables** can be used **with a maximum deviation of 5%** as shown in Table 2.9. The **E**xponential **F**it **N**ear **O**pening **G**ap is an accurate method, but it can only be used for single-particle gap and excitation gap. In the currently published paper by Gebhard et. al (2022), the critical point $V_{cdw} = 2$ is determined with an accuracy of 7.5% using the

Exponential **F**it **N**ear **O**pening **G**ap method applied to single-particle gap. In this work, an accuracy of **less than 3%** was achieved using this method.

A much better method, which achieves an even higher **accuracy of 2.5%**, is the **P**hase **I**ndependent **F**it method. As the study of the 1DSF chain has shown, it was possible to apply it successfully not only to the single-particle gap, but also to excitation gap, and entropy and that for different parity (even, odd) and CCS symmetry.

Observable	Method	Parity [CCS]	V_c	Deviation
S	**P**hase **I**ndependent **F**it	Odd [both]	2 ± 0.05	2.5%
c	Zero crossing	(Odd, Even) [yes]	2.08 ± 0.01	4.5%
ΔE	**E**xponential **F**it **N**ear **O**pening **G**ap	Odd [yes]	2.01 ± 0.06	3.5%
ΔE	**P**hase **I**ndependent **F**it	Even [both]	2 ± 0.05	2.5%
ΔE	**P**hase **I**ndependent **F**it	Odd [no]	2 ± 0.05	2.5%
ΔE	**E**xtremum in a **F**inite **S**ystem	Even [both]	2.05 ± 0.05	5%
E_p	**E**xponential **F**it **N**ear **O**pening **G**ap	Even [both]	1.945	2.75%
E_p	**E**xponential **F**it **N**ear **O**pening **G**ap	Odd [yes]	1.928	3.65%

Table 2.9: Summary of the best observables and applied methods to determine the critical point of the 1DSF chain with a maximum deviation of 5%.

3. RESULTS FOR 2-LEG LADDER

In the following, a **homogeneous 2-leg ladder** is investigated in an analogous way. For this ladder, the interaction potential along the rungs and legs is set equal: $V = V_x = V_y$. The **ladder length** L is the number of lattice sites of *one* leg. The **total number** of lattice sites is $2L$. The ladder is filled with L **spinless fermions** (half-filling case).

The observables from Chapter 1.6 are investigated as a function of the **interaction potential** V and as a function of the ladder length L, and an attempt is made to extract the **theoretically predicted critical value** at $V_{cdw} = 0$ of an infinite ladder.

Although a 2-leg ladder generally requires a larger dimension m for DMRG, in this work the dimension $m = 100$ is used as for the 1DSF model and only the number of sweeps is increased to 12. The difference of the **exact ground state energy** $E_{0,\text{exact}}$ calculated with Eq. (1.1) of a *non-interacting* $(V = 0)$ ladder and the **simulated ground state energy** $E_0(m = 100)$ yields the **convergence error**: $\left|E_{0,\text{exact}} - E_0(m = 100)\right| \approx 0.008$ for $L = 400$. This accuracy is also assumed for an *interacting* ladder $(V > 0)$.

Theoretically, it should not make any difference in the simulations whether the ladder length L is chosen as even or odd, because the *total* number of lattice sites $2L$ of a two-leg ladder is *always even*. Therefore, the simulation of a ladder of length L and $L + 1$ is expected to differ only because of the different number of fermions: N and $N + 1$ or because the observable exceeds the order of the convergence error.

3.1. ENTANGLEMENT ENTROPY

The **entanglement entropy** $S(L)$ of a 2-leg ladder as a function of the ladder length L, for *even*/*odd* length *with*/*without* CCS, behaves like a 4th degree polynomial function near the theoretical phase transition $V_{\mathrm{cdw}} = 0$ (see Figure 3.1):

$$S(L) = AL^4 + BL^3 + CL^2 + DL + S_\infty \tag{3.1}$$

Thus, in contrast to the 1DSF model, $S(L)$ of a 2-leg ladder does not exhibit two different behaviors (logarithmic and polynomial 2nd degree). Therefore, the **P**hase **I**ndependent **F**it method for extracting the critical value, which works excellently for the entropy of the 1DSF chain, could not be applied to the entropy $S(L)$ of a 2-leg ladder. This is because this method only works if an observable exhibits two different functional behaviors, depending on the choice of V. In the critical range $-1 < V < 1$, however, $S(L)$ exhibits only a *single* behavior (3.1). Therefore, the entropy $S(L)$ of a 2-leg ladder is not suitable for the extraction of the critical value.

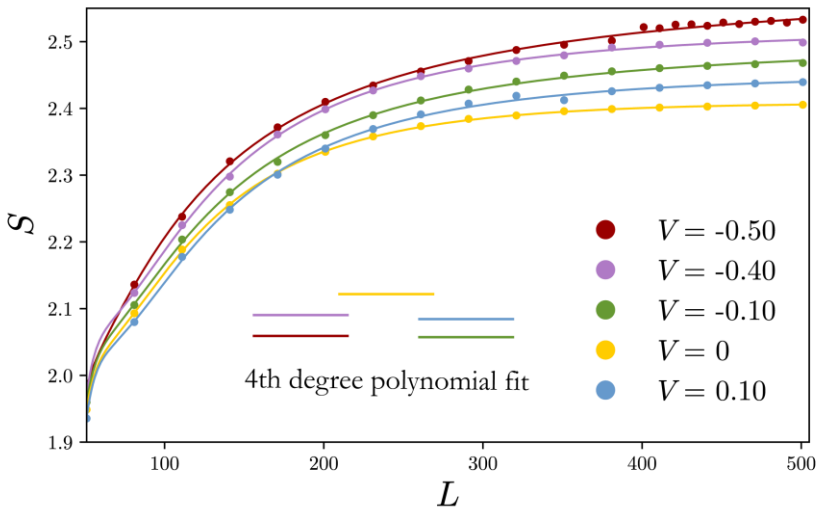

Figure 3.1: Entropy $S(L)$ of an odd 2-leg ladder with CCS as a function of L for various interaction potentials V. Solid line is a polynomial fit.

In the thermodynamic limit $L \to \infty$, the entropy $S(L)$ converges toward a constant value $S_\infty(V)$ (for all V) which depends on V. The convergence of $S(L)$ toward a fixed value, is also observed in the CDW phase of the 1DSF model.

Simulation of entropy $S(V)$ as a function of V shows similar behavior to an *odd* 1DSF chain *with* CCS, but the $S(V)$ curves of a two-leg ladder are shifted more to the left, to smaller V, as Figure 3.2 shows. This suggests that the phase transition to a CDW phase in a ladder happens at smaller interaction potential. The inset of Figure 3.2 also shows

that the entropy $S(V)$ *approaches zero* exponentially in the limit $V \to \infty$ and can be fit with Eq. (1.23).

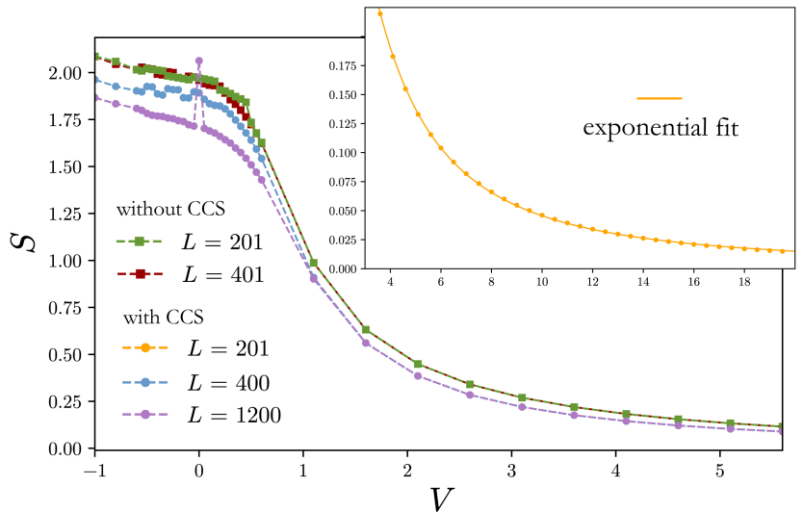

Figure 3.2: Entropy $S(V)$ of a 2-leg ladder with/without CCS as a function of V for various lengths. The inset shows that entropy for large V.

3.2. CENTRAL CHARGE

The **magnitude $|c(V)|$ of the central charge** of a finite 2-leg ladder is shown as a function of V in Figure 3.3. There (L, L') = (odd, odd) length combinations are shown which worked well for a 1DSF chain.

- For $V \gtrsim 0.9$, central charge is zero and the ladder is thus in the CDW phase for this parameter range.
- For $V < 0.9$, central charge fluctuates strongly between $|c(V)| = 0$ and $|c(V)| \approx 0.6$. Here, the CDW phase is poorly formed. The fluctuation in $|c(V)|$ is due to the fluctuation of the entropy $S(V)$ in this range (see Figure 3.2).
- According to the **C**onformal **F**ield **T**heory, $|c| = 0$ in the CDW phase, so the critical value here *seems* to be $V_c \approx 0.9$. Also, other length combinations (L, L') *with* or *without* CCS do not provide a better prediction for the theoretical critical value at $V_{cdw} = 0$ of an infinite ladder.

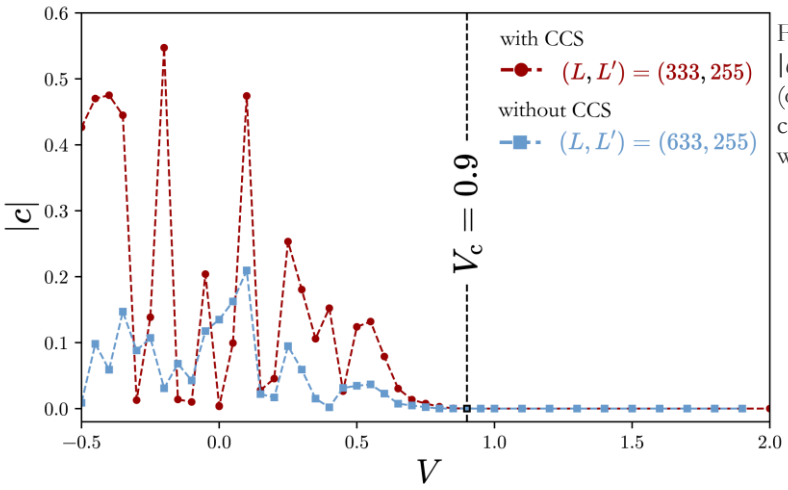

Figure 3.3: Central charge $|c(V)|$ of a 2-leg ladder for (odd, odd) length combination with and without CCS.

3.3. EXCITATION GAP

The excitation gap $\Delta E(V)$ as a function of V for a 2-leg ladder is shown in Figure 3.4.

- For $V \geq 1.2$, the **excitation gap is zero** for all parities *with/without* CCS as it is for an infinite ladder because of the twofold degeneracy of the ground state in the CDW phase $V \geq 0$.[1] However, the simulated excitation gap is small but nonzero for $0 \leq V < 1.2$, which distinguishes it from the result in the thermodynamic limit.
- For $V < 1.2$, the degeneracy of the ground state is slightly eliminated. The **non-vanishing of the excitation gap** is also observed for the 1DSF chain and exploited to estimate the critical value based on the extremum that occurred. For $\Delta E(V)$ of a 2-leg ladder, extrema near $V_{\text{cdw}} = 0$ also occur, but not unique ones as is the case for the 1DSF chain. Rather, the extrema look like a sequence of fluctuations that occur because of reaching the order of the DMRG convergence error. One can really speak of fluctuations, since a repeated simulation of the excitation gap with unchanged parameters yields small changes in this interaction range.
- In the CDW phase, the ground state is degenerate, so the excitation gap must vanish in this phase. The phase transition to a CDW seems to occur at $V_c \approx 1.2$.

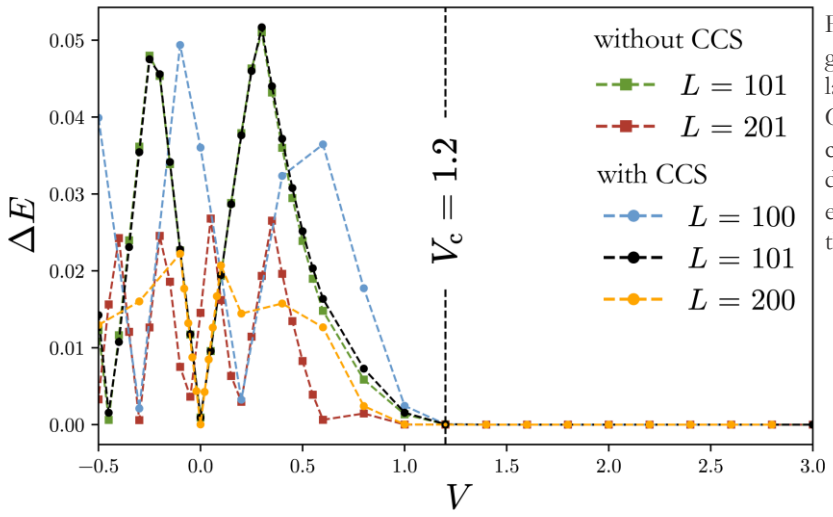

Figure 3.4: Excitation gap $\Delta E(V)$ for a 2-leg ladder with and without CCS. The determined critical value $V_c \approx 1.2$ differs strongly from the exact value $V_{cdw} = 0$ in thermodynamic limit.

3.4. SINGLE-PARTICLE GAP

The **single-particle gap** $E_p(V)$ of a 2-leg ladder as a function of the interaction potential V exhibits a similar behavior to the single-particle gap of a 1DSF chain from Chapter 2.4:

- For $V \gg 1$, the gap $E_p(V)$ of an *even/odd* ladder length *with/without* CCS grows linearly.
- For $V < 1$, the gap $E_p(V)$ approaches zero. Since the gap becomes very small here and may exceed the convergence error, it exhibits fluctuations when zoomed in near the critical region (see inset of Figure 3.5).

- The gap opens exponentially near the critical region for ladders *with* CCS. Therefore, the **E**xponential **F**it **N**ear **O**pening **G**ap method is suitable here. Since the gap fluctuates at small V and the exponential fit (1.23) is poor or not possible, the fit is always started from $\underline{V} = 0.9$ and carried out up to $\overline{V} = 4$. With this choice of fit limits, the gap of a ladder *without* CCS **deviates from the exponential behavior**, as shown in Figure 3.5 but still provides an accurate critical value.

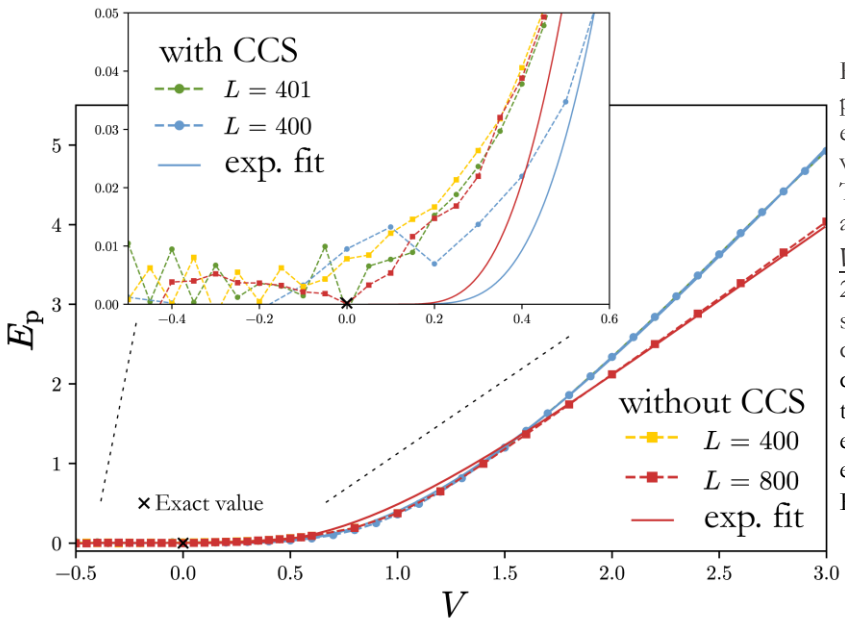

Figure 3.5: Single-particle gap for even/odd ladder lengths with and without CCS. The exponential fit is always made between $\underline{V} = 0.9$ and $\overline{V} = 4$ for 2-leg ladders. The inset shows the magnified critical region. Here one can see (in some cases) the deviation from the exact ground state energy calculated with Eq. (1.11) at $V = 0$.

Table 3.1 summarizes the **critical values** V_c determined using the **E**xponential **F**it **N**ear **O**pening **G**ap method. The gaps of *even*/*odd* ladder lengths *without* CCS are almost identical even when zoomed in on the critical region, and they yield the same critical value of $V_c = 0.05$, deviating from the exact theoretical value $V_{cdw} = 0$ in the thermodynamic limit by 5%. The gap of *even* and *odd* ladder lengths *wit*h CCS deviates slightly from each other near the critical region, possibly due to convergence errors on this small scale.

Furthermore, the single-particle gap $E_p(V)$ as a function of V in the investigated length range $200 \leq L \leq 800$ is independent of the length for $V \gg 1$. For $V \ll 1$ on the other hand, the gap shows a slight dependence on the length. However, the fluctuations are within the magnitude of the convergence error, which is why the finite-size scaling $E_p(L)$ of the single-particle gap does not provide a meaningful result. The application of the **P**hase **I**ndependent **F**it method requires a more accurate determination of the single-particle gap.

Method	Parity [CCS]	V_c
Exponential **F**it **N**ear **O**pening **G**ap	Even [yes]	0.23
Exponential **F**it **N**ear **O**pening **G**ap	Even/Odd [no]	0.05
Exponential **F**it **N**ear **O**pening **G**ap	Odd [yes]	0.05

Table 3.1: Summary of the results using single-particle gap to determine the critical value V_c of an infinite 2-leg ladder with an exact critical value $V_{cdw} = 0$.

3.5. CDW ORDER PARAMETER

The **CDW order parameter** $\delta(V)$ of a 2-leg ladder as a function of V, as shown in Figure 3.6, is independent of the ladder length in the investigated length range. A slight length dependence only arises when zooming in close to the theoretical phase transition at $V_{cdw} = 0$ (see inset of Figure 3.6). Since the order parameter in this range is of the same magnitude as the convergence error, it is not clear whether this length independence is actually a physical effect or not. Due to this length independence, the investigation of the finite-size scaling $\delta(L)$ of the order parameter is meaningless.

The simulation of the order parameter $\delta(V)$ of a finite 2-leg ladder as a function of V exhibits the following behavior.

- **For large interaction potentials** $V \gg 1$: Regardless of the parity of the chain length or the CCS symmetry, the magnitude $|\delta(V)|$ approaches 0.5. The same behavior is also observed for a 1DSF chain of *odd* length *with* CCS.
- **For small interaction potentials** $V \lesssim 1$: The order parameter increases monotonically from the value $\delta = 0$, starting at $V \approx -1$. This means that the CDW phase already forms for a *finite* chain for a *negative* interaction potential, deviating from the theoretically predicted case for an infinite ladder. In the latter case, the CDW phase starts to form at $V_{cdw} = 0$.

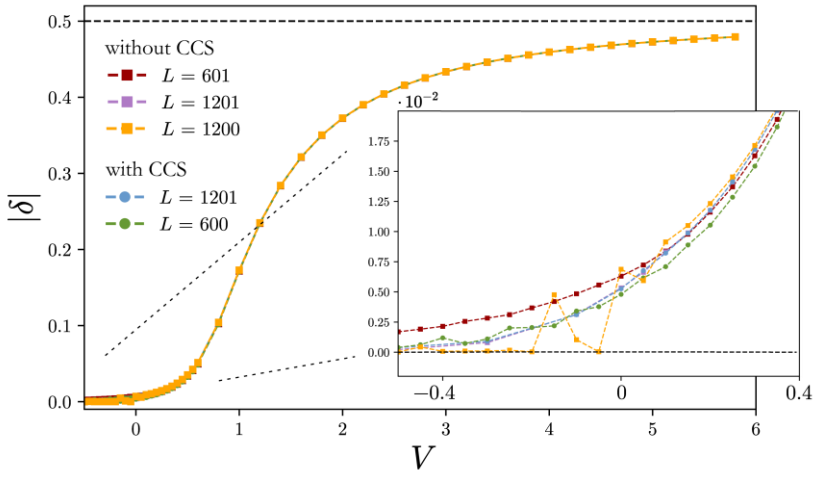

Figure 3.6: CDW order parameter for even/odd ladder lengths with and without CCS. The inset shows the magnified critical region.

The order parameter $\delta(V)$ is also in the case of a finite 2-leg ladder a poor *quantitative* indicator for a theoretically occurring phase transition at $V_{\mathrm{cdw}} = 0$ in the thermodynamic limit. Thus, an accurate determination of the critical value with the order parameter is not possible. For the quantitative determination of the critical value, the density fluctuation discussed in the following chapter is better suited. Nevertheless, the order parameter $\delta(V)$ shows *qualitatively* similar behavior to the theory, independent of parity and CSS symmetry.

3.6. Density Fluctuation

The **density fluctuation** $\sigma^2(V)$ of a 2-leg ladder as a function of V is shown in Figure 3.7. It shows, just like the CDW order parameter, a minor length dependence in the vicinity of the critical region: $-1 < V < 1$.

- **For large interaction potentials** $V \gg 1$: Regardless of the parity of the chain length or the CCS symmetry, the magnitude $\sigma^2(V)$ approaches 0.25. The same behavior is also observed for a 1DSF chain of *odd* length *with* CCS.
- **For small interaction potentials** $V \lesssim 1$: Something happens here that was not observed with the CDW order parameter. The density fluctuation is approximately zero. But, when zoomed into this region, a **minimum** V_c can be observed near $V = 0$ - assuming the ladder has no CCS symmetry (see inset of Figure 3.7). Because of the slight length dependence of the density fluctuation $\sigma^2(V)$ in this region, the position of the minimum also varies with ladder length. Table 3.2 summarizes the minima for different ladder lengths L.

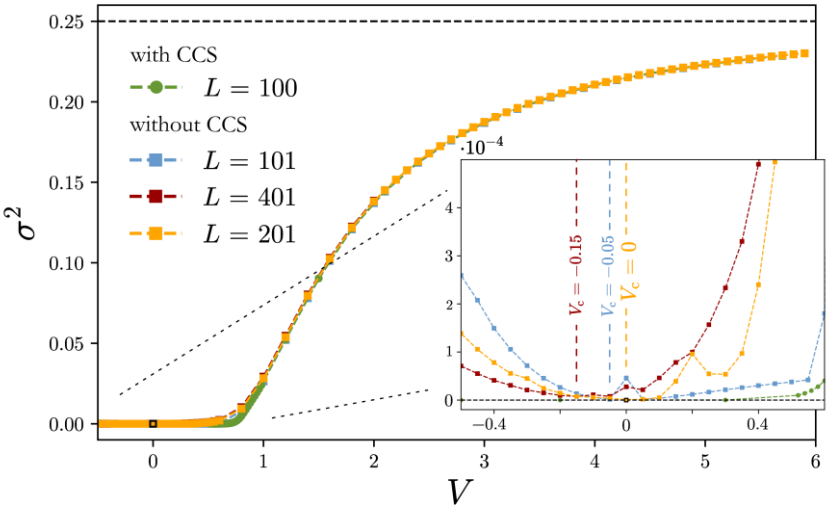

Figure 3.7: Density fluctuation for even/odd ladder lengths with and without CCS. The inset shows the magnified critical region with occurring minima.

L	V_c
101	-0.05 ± 0.06
201	0.0 ± 0.06
401	-0.15 ± 0.06

Table 3.2: Position of the minimum V_c in the density fluctuation $\sigma^2(V)$ for different lengths L of a 2-leg ladder without CCS. The minima are interpreted as critical values.

3.7. DENSITY-DENSITY CORRELATION FUNCTION

The **density-density correlation function** $|F(x)|$ has already given results difficult to interpret for the 1DSF chain. For the 2leg ladder, the interpretation is even more difficult. Figure 3.8 shows an example result for the correlation function of a 2leg ladder of length $L = 100$ *without* CCS with respect to the site $x_0 = 1$:

- For $V \gtrsim 1$ the correlation function oscillates, where the **amplitude is independent of** x, but increases with larger V.
- For $V = 0$ the correlation function is **constant** $|F(x)| = 0.25$ for all x.
- For $V \lesssim 1$ the correlation function oscillates as for the case $V \gtrsim 1$, but the **oscillation is very small** and only visible after zooming in (see inset of Figure 3.8). The amplitude here **decreases from the edge to the center** of the ladder, but neither exponentially nor according to the power law. This makes the interpretation of the correlation function difficult.

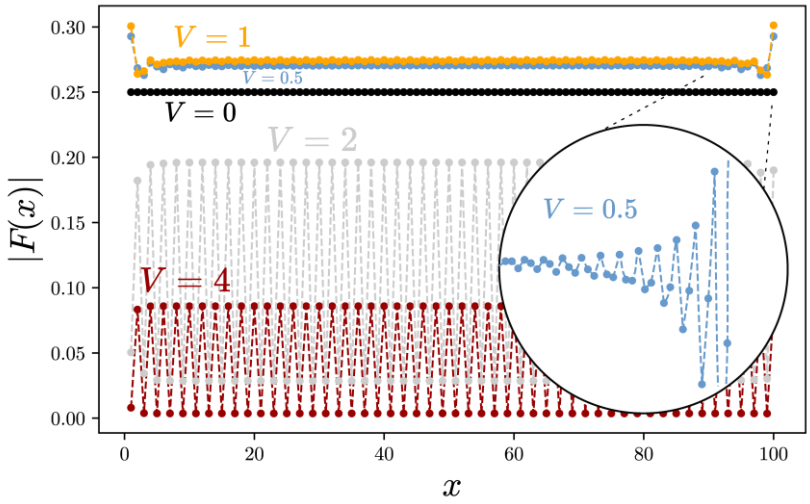

Figure 3.8: Correlation function $|F(x)|$ with $x_0 = 1$ for different V. A ladder of length $L = 100$ without CCS was used. Das Inset zeigt die The inset shows the edge oscillations at $V = 0.5$.

This observable will not be investigated further. Enough methods and other observables have already been tested that provide detection of the critical point and information about the different phases. It is also possible that I simply made a mistake in the code implementation of the correlation function... In a further work the problem with the correlation function can be approached more closely.

3.8. SUMMARY

Three of the studied observables, the **single-particle gap E_p, CDW order parameter δ**, and the **density fluctuation σ^2** of a 2-leg ladder, **show similar behavior to the 1DSF chain**. Unfortunately, the order parameter, entropy, central charge and correlation function were not useful in determining the critical value. In contrast, the **E**xponential **F**it Near **O**pening **G**ap method **works well even for a 2-leg ladder**. However, even those methods that have provided an accurate critical value, such as single-particle gap, should be viewed with caution. The very small single-particle gap in the vicinity of the phase transition is *in the order of the convergence error*. This leads to fluctuations in the critical region and prevents, for example, the use of the **P**hase **I**ndependent **F**it method.

The density fluctuation σ^2 of a 2-leg ladder *without* CCS shows a slightly noticeable **minimum** when zooming in **near the critical region**, which did not occur in a 1DSF chain. This minimum seems to be slightly length dependent, but still provides a **fairly accurate critical value of the ladder** in the thermodynamic limit as shown in Table 3.3.

If the accuracy of the observables can be improved (by decreasing the convergence error), the **P**hase **I**ndependent **F**it method can also be applied to a 2-leg ladder. But even with a smaller convergence error, the study of the 2-leg ladder is more complex than that of the 1DSF chain, and the **methods that worked for the chain only partially work for the ladder**. It was this observation in Ref. 6 that motivated the present systematic study observables and methods. The following Table 3.3 summarizes the best methods and observables for determining the critical value of a 2-leg ladder.

Observable	Method	Parity [CCS]	V_c
E_p	**E**xponential **F**it **N**ear **O**pening **G**ap	Odd [yes]	0.05
E_p	**E**xponential **F**it **N**ear **O**pening **G**ap	Even/Odd [no]	0.05
σ^2	**E**xtremum in a **F**inite **S**ystem	Odd [no]	0.0 ± 0.06

Table 3.3: Summary of the best observables and applied methods to determine the critical point V_c of a 2-leg ladder.

4. RESULTS FOR AN ALTERNATING 1221-LADDER

In the following, the most important system of this work is investigated, namely an **alternating 1221 ladder**. It is a periodic arrangement of the sites as shown in Figure 1.9. The **interaction potential** V between all sites is equal. The ladder length is $4m$ with $m = 1,2,3, \ldots$ The **total number of sites** $L = 6m$ is always a multiple of six. A half-filled ladder has $N = L/2 = 3m$ spinless fermions. The observables from Chapter 1.6 are studied as a function of the interaction potential V and as a function of the total number of sites L.

The difficulty in studying a half-filled 1221 ladder is that **no exact solution** in thermodynamic limit exists, so the numerical results cannot be compared with theory. However, something can be stated *numerically* about the limiting cases $V = 0$ and $V \to \infty$:

- In the limiting case $V = 0$ of **non-interacting fermions**, the 1221 ladder is a band insulator[16] in which the lowest excitations are unbound particle-hole pairs. The energy gap ΔE remains the same for a band insulator as the ladder size L increases, as will be evident in Chapter 4.2. The ground state is non-degenerate, so the excitation gap ΔE coincides with the single-particle gap: $\Delta E = E_{\mathrm{p}}$.

- In the limiting case $V \to \infty$ of an **infinitely large repulsion**, the fermions take the largest possible distance to each other. A **C**harge **D**ensity **W**ave with a *twofold degenerate* ground state is formed, as shown in Figure 4.1. This results in the excitation energy $\Delta E = E_1 - E_1 = 0$ and the energy gap $E_\mathrm{p} = V$, as observed for the 1DSF chain and 2-leg ladder.

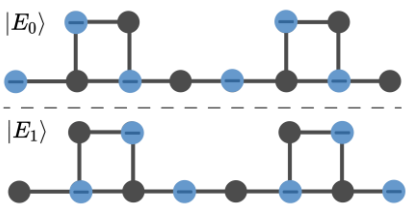

Figure 4.1: Two degenerate states of a 1221 ladder in the $V \to \infty$ limit.

The question now is whether there is another phase between the band isolator at $V = 0$ and the CDW phase at large V:

- **If THERE IS another phase**, it is necessary to find out what that specific phase is and where its boundaries are to the band isolator and CDW phase.
- **If THERE IS NO other phase**, it must be found out at which critical value V_c the phase transition from the band insulator to the CDW phase happens. It must also be checked numerically whether the second phase is actually a CDW phase. This will be indicated in particular by the non-vanishing CDW order parameter. It would also be interesting to know whether the phase transition is first order (abrupt) or second order (continuous).

The **dimension** m of the left DMRG block is set to 100 and the **number of sweeps** to 12. This choice of parameters provides good, consistent results, as will be evident in subsequent chapters. As with the 2-leg ladder, the number of sites is *always even* because of the structure of the 1221 ladder.

4.1. Entanglement Entropy

Figure 4.2 shows the **entropy** $S(V)$ of a 1221 chain *with*/*without* CCS as a function of the interaction potential V. In contrast to the previously studied systems, the entropy of a *finite* 1221 chain *with* CCS shows a length-independent **discontinuity near** $V = 2$. The 1221 chain *without* CCS on the other hand shows a length-dependent **maximum near** $V = 2$. *Linear* extrapolation of the maximum position $V_\mathrm{c}(1/L)$ as a function of $1/L$ yields the critical value in the thermodynamic limit: $V_\mathrm{c}(1/L = 0) \approx 2.15$ (*without* CCS) and $V_\mathrm{c}(1/L = 0) \approx 2.05$ (*with* CCS). See Figure 4.11 for demonstration. The entropy $S(V)$

therefore provides a first sign that a phase transition is taking place at the discontinuity point.

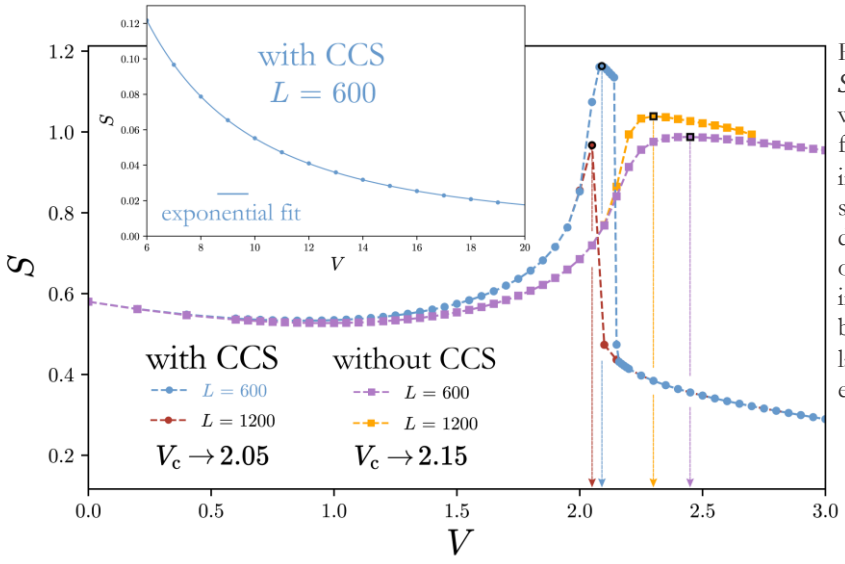

Figure 4.2: Entropy $S(V)$ of a 1221 ladder with/without CCS as a function of the interaction potential V shows either a length-dependent discontinuity or an extremum. The inset shows the behavior of entropy for large V, which decays exponentially.

Second sign is that the entropy $S(V)$ of a 1221 ladder as a function of V shows the same behavior in the limit $V \to \infty$ as the entropy of a 2-leg ladder (Figure 3.2) - it **goes exponentially to zero** (inset of Figure 4.2). The entropy can be fitted with the same function (1.23) as the single-particle gap near the phase transition. But also the entropy $S(L)$ as a function of L of a 1DSF chain (Figure 2.1) and a 2-leg ladder (Figure 3.1) *in the CDW phase* **move towards a constant entropy** in the limit $L \to \infty$. This behavior of the entropy $S(L)$ is also observed for a 1221 ladder *with* CCS, as Figure 4.4 shows. Like the 2-leg ladder, it can be fitted with the 4th degree polynomial function (3.1).

The third sign indicating a phase transition is the behavior of the **exponent** $|\kappa(V)|$ as a function of V from the **P**hase **I**ndependent **F**it method. Figure 4.3 shows the exponent $|\kappa(V)|$ as a function of V extracted from the finite-size scaling of the entropy (see inset of Figure 4.4):

- For a 1221-ladder *with* CCS and $V \leq 2.04$ the exponent is zero up to the 5th decimal place. The exponent also vanishes for a ladder *without* CCS in this region.
- At $V = 2.05$ (ladder *with* CCS), a sharp peak occurs suggesting a phase transition in the thermodynamic limit near this point. For a ladder *without* CCS, the peak is broadened and shifted to $V = 2.21$.
- For $V > 2.05$ (ladder *with* CCS) the exponent decreases rapidly to $|\kappa(V)| = 0$. For a ladder *without* CCS, the decay to $|\kappa(V)| = 0$ is slower, but neither exponential, power law nor polynomial of 4th order.

The *insulating* CDW phase of the 1DSF chain was characterized by $|\kappa(V)| = 0$. In contrast, the *conducting* **L**uttinger **L**iquid phase was characterized by $|\kappa(V)| = 1$.

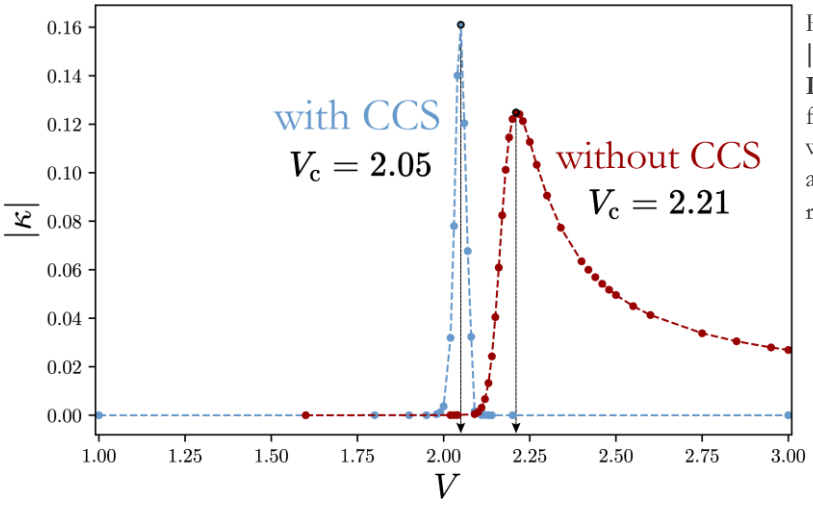

Figure 4.3: The exponent $|\kappa(V)|$ from the **P**hase **I**ndependent **F**it method for a 1221 ladder with/without CCS shows a maximum V_c in the region $2.04 \leq V_c \leq 2.22$.

Therefore, it seems that a phase transition between *two insulating* phases occurs in the 1221 chain because the exponent vanishes in both phases.

These observations suggest that a phase transition *from an insulating to an insulating* phase occurs near $V \approx 2$. Whether this is in fact a phase transition *to a CDW phase* will become clear after the subsequent observables are analyzed.

The following Table 4.1 summarizes the methods that, applied to entropy, reveal a possible phase transition in a 1221 ladder in the thermodynamic limit. According to the applied methods, the critical value lies somewhere in the region: $2.04 \leq V_c \leq 2.22$.

Method	CCS	V_c
Linear Extrapolation of **E**xtrema in $S(V)$ of a **F**inite **S**ystem	Yes	≈ 2.05
Linear Extrapolation of **E**xtrema in $S(V)$ of a **F**inite **S**ystem	No	≈ 2.15
Phase **I**ndependent **F**it	Yes	2.05 ± 0.01
Phase **I**ndependent **F**it	No	2.21 ± 0.01

Table 4.1: Methods for determining the possible critical value in a 1221 ladder applied to entropy. How the error of V_c is determined is described at the end of Chapter 2.1.

According to the **C**onformal **F**ield **T**heory, the **central charge** $c(V)$ as a function of the interaction potential V in the case of a 1DSF chain is a quantity which, depending on the value, characterizes a *metallic* phase $(c = 1)$ or an *insulating* phase $(c = 0)$ in the thermodynamic limit. It is possible to calculate the central charge $c(V)$ also for a 1221 ladder. For this purpose, the entropy is calculated for two different numbers of sites (L, L') as described in Chapter 1.6.2 and then Eq. (1.14) is used.

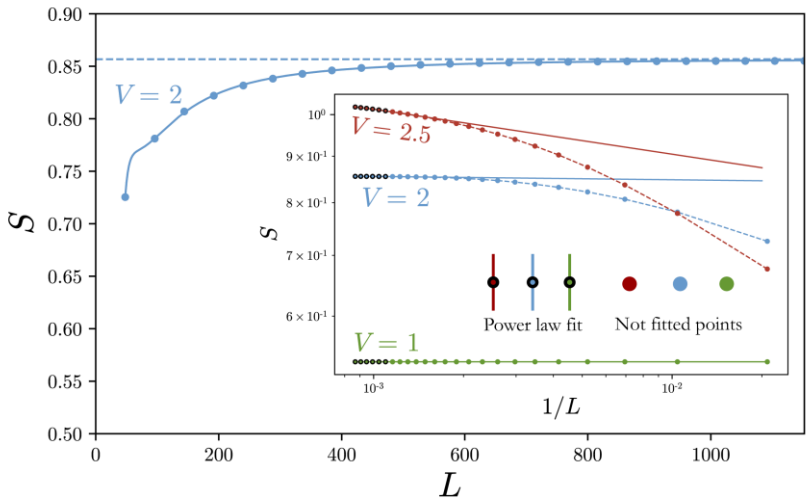

Figure 4.4: Entropy $S(L)$ of a 1221 ladder with CCS as a function of the number of sites L saturates rapidly at the entropy value $S_\infty(V)$ that is dependent on V. The same behavior is observed for a 1221 ladder without CCS. The inset shows the power law fit of six black points representing the largest lengths. These fits are used for the **P**hase **I**ndependent **F**it method.

Figure 4.5 shows the central charge $c(V)$ as a function of V for different, arbitrarily chosen, number of sites combinations $(420, 402)$, $(600, 402)$ and $(1200, 600)$. As can be seen, the combination $(420, 402)$ cannot be interpreted with the above explanation and this combination also does not exhibit any feature close to $V = 2$, as was the case with entropy. However, this situation changes when the difference $L' - L$ is increased:

- For the combination $(600, 402)$ of a 1221 ladder *with* CCS, a **maximum occurs at** $V_c = 2.07 \pm 0.01$.
- For the combination $(600, 402)$ of a 1221 ladder *without* CCS no maximum is seen, but it occurs at a larger difference - here at $(1200,600)$. The **maximum is at the position** $V_c = 2.17 \pm 0.01$.

Furthermore, independent of CCS symmetry, the central charge of a 1221 ladder indicates that with the larger difference $L' - L$, the **central charge converges to zero** on both sides of the maximum. According to the **C**onformal **F**ield **T**heory, it suggests a phase

transition near $V \approx 2$ from one *insulating* phase to another *insulating* phase in the thermodynamic limit.

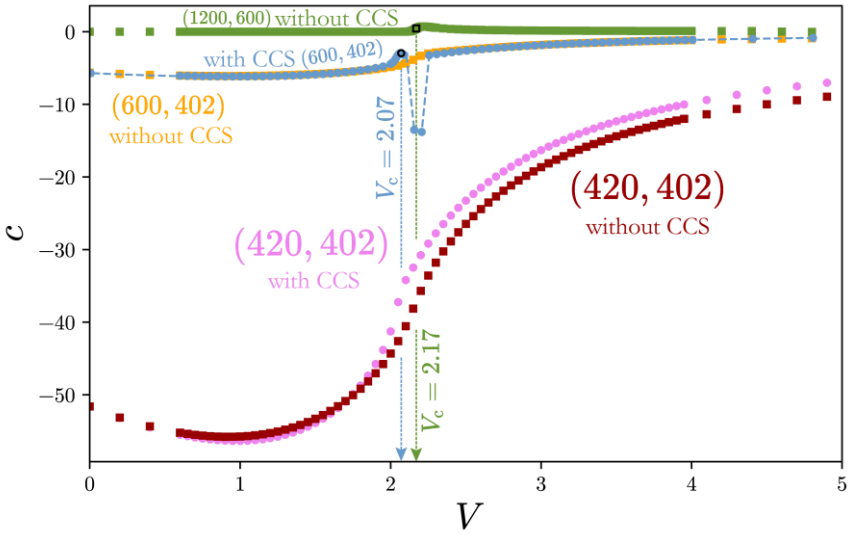

Figure 4.5: Central charge $c(V)$ of a 1221 ladder as a function of the interaction potential for different number of sites combinations (L, L') with/without CCS. An extremum occurs at $V_c = 2.07$ (with CCS) and at $V_c = 2.17$ (without CCS).

In addition, the central charge confirms the predictions about the position of the critical value done by the entropy. However, since central charge is closely related to entropy via Eq. (1.14), it is not surprising that they show similar results. It is also worth noting that the central charge shows a **local minimum near** $V \approx 1$ that has also occurred in the entropy. Whether this is a special point in the thermodynamic limit or just a finite-size effect will become clear in the following chapters.

4.2. Excitation Gap

The **excitation gap** $\Delta E(V)$ of a 1DSF chain *without* CCS as a function of V has shown a *length-dependent* maximum that shifted toward the theoretical phase transition $V_{cdw} = 2$ as the chain length increased (see Chapter 2.3). The excitation gap $\Delta E(V)$ of a 1221 ladder *with/without* CCS also has a **maximum** $V_{max} \approx 0.2$, which, however, is *independent of length*, as shown in Figure 4.6. This maximum did not occur in either the entropy or the central charge of the 1221 ladder and is therefore assumed to be a finite-size effect. The **maximum near** $V = 2$ is much more interesting, because it also occurred in the study of entropy and central charge.

The excitation gap of the 1221 ladder *with* and *without* CCS differ slightly in the region $1 < V < 2.5$, which is why the maximum near $V = 2$ is also different (see Figure 4.6):

- For the 1221 ladder *with* CCS, the excitation gap decreases to zero and has a **discontinuity at the position** $V_c \approx 2.05 \pm 0.05$. The abruptness and the slight length dependence of the discontinuity can be seen more clearly when the excitation gap is plotted on a logarithmic scale (inset of Figure 4.6).
- For the 1221 ladder *without* CCS, the excitation gap **decreases continuously** and is zero to the fourth decimal place starting at $V \geq 2.55$.

Even though the excitation gap *with* CCS has a special point at $V = 2.05$, however, it depends on the arbitrary choice with which accuracy the excitation gap is considered to be zero. Here it is considered as $\Delta E = 0$, if it is less than $|\Delta E| < 10^{-3}$. The vanishing of the excitation gap starting at $V = 2.05$ provides a **first hint** for the degeneracy of the ground state and thus a necessary condition **for the CDW phase**.

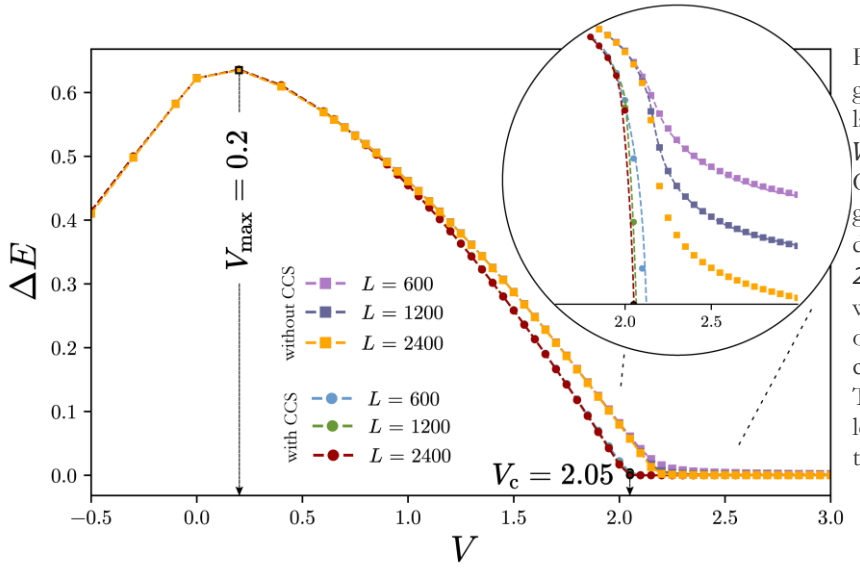

Figure 4.6: Excitation gap $\Delta E(V)$ of a 1221 ladder as a function of V. The ladder with CCS has an excitation gap with a discontinuity at $V = 2.05$. The ladder without CCS, on the other hand, decreases continuously to zero. The inset is a logarithmic scaling of the critical region.

One way, **free from arbitrariness**, to quantitatively determine this special point near $V = 2$ is the **P**hase **I**ndependent **F**it method. As Figure 4.7 shows, the associated **exponent** $|\kappa|$ **has a maximum at** $V_c = 2.07 \pm 0.01$ for the ladder *with* CCS. Investigation of the energy gap ΔE of the ladder *with* CCS confirms the predictions of the previous observables that a phase transition must be somewhere between $2 \leq V_c \leq 2.1$.

In contrast, the $|\kappa|$ exponent of a 1221 ladder *without* CCS has no maximum, but **become non-zero at** $V \approx 2$ and **goes monotonically toward** $|\kappa| \to 2$ for $V \to \infty$. The same behavior of the exponent was observed for the single-particle gap of the 1DSF chain *without* CCS (see Figure 2.17). It seems that the exponent $|\kappa| = 2$ is equivalent to $|\kappa| = 0$. Whether this conjecture is true needs to be investigated in another work.

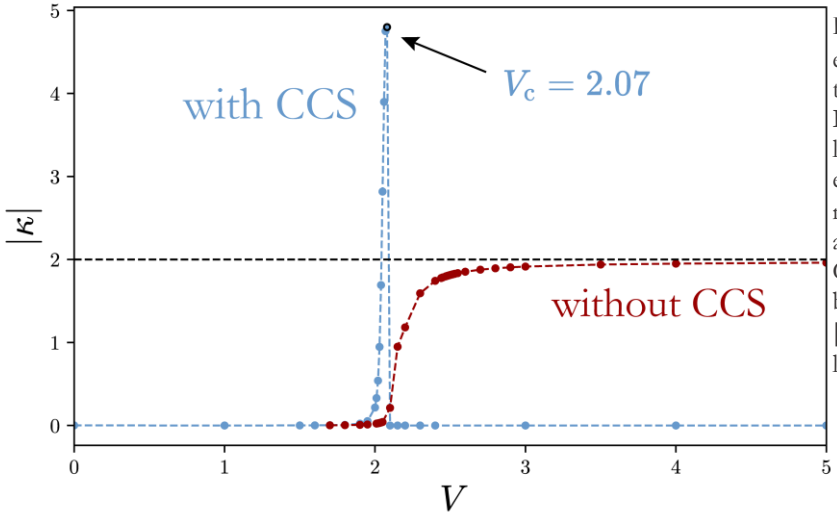

Figure 4.7: The exponent $|\kappa(V)|$ from the **P**hase **I**ndependent **F**it method for a 1221 ladder with CCS using excitation gap shows a maximum $V_c = 2.07$ and a ladder without CCS has no maximum, but saturates at $|\kappa(V)| = 2$. Dashed line is for eye-guidance.

Moreover, the **P**hase **I**ndependent **F**it method applied to the excitation gap ΔE of a 1221-ladder *with* CCS implies two things:

1. The **maximum at $V_{max} = 0.2$** that occurred in the excitation gap $\Delta E(V)$ as a function of V is in fact **only a finite-size effect** and will not (if true) occur in the thermodynamic limit of the 1221 ladder.
2. On the left and on the right of the maximum (with a small distance to it), the **exponent is $|\kappa| = 0$**, which indicates a **phase transition between two isolating phases**.

It is surprising that all three observables of a 1221 ladder with CCS investigated so far provide an indication of a phase transition near $V = 2$. The **P**hase **I**ndependent **F**it method stands out especially with its *unambiguous* predictions.

4.3. SINGLE-PARTICLE GAP

The **single-particle gap $E_p(V)$** of a 1DSF chain and a 2-leg ladder **is linear in the CDW phase** for large V (see Figure 2.13 and Figure 3.5). This behavior is also observed for the single-particle gap $E_p(V)$ of a 1221 ladder *with/without* CCS, as Figure 4.8 shows. Note, however, that linearity is not a sufficient condition for the CDW phase to occur. However, in combination with the vanishing excitation gap ΔE, they imply a degeneracy of the ground state, which also occurs in the CDW phase. Furthermore, it can be seen that the 1221 ladder *with* CCS shows a **minimum at $V_c = 2.05$** and provides further evidence that a phase transition occurs close to this point.

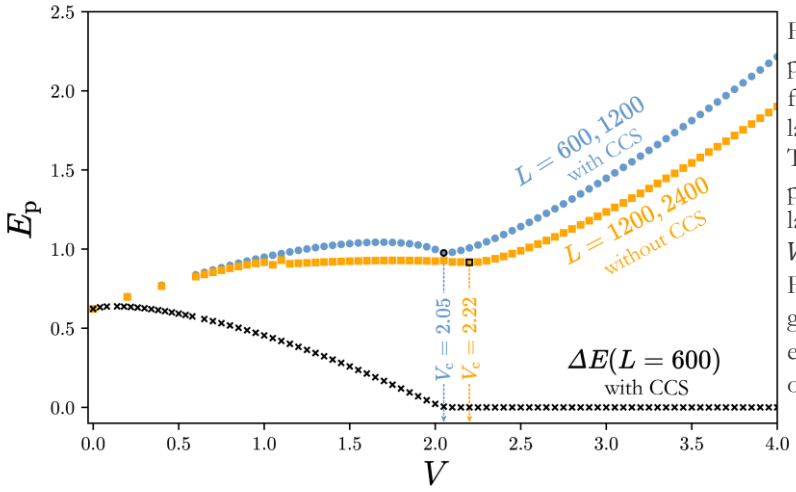

Figure 4.8: The single-particle gap $E_p(V)$ as a function of V for a 1221 ladder with/without CCS. There is an extremum at the point $V_c = 2.05$ for the ladder with CCS and at $V_c = 2.22$ without CCS. For $V > 2.5$, the energy gap is linear. E_p and excitation gap ΔE coincide only at $V = 0$.

For $V \leq 2$, the gap differs from that of a 1DSF chain. While the single-particle gap of the 1DSF chain vanishes in the metallic phase $(V \leq 2)$, the length-independent single-particle gap of the 1221 ladder *with* CCS is non-zero in this region. It first increases linearly, saturates and drops again to a minimum, and then increases linearly again. The length-independent gap of the 1221 ladder *without* CCS differs in that it does not produce a pronounced minimum. It only becomes visible at $V_c = 2.22$ after zooming in. However, both ladders (*with*/*without* CCS) have two things in common:

1. As described and expected in the introduction of Chapter 4, the single-particle gap E_p of a *non-interacting* 1221 ladder $(V = 0)$ coincides with the excitation gap ΔE. This confirms that the **non-interacting 1221 ladder is a band insulator** regardless of the CCS symmetry.
2. For $0 < V < V_c$, excitation gap ΔE does not coincide with the single-particle gap E_p. So the ladder can not be a **band insulator** in this region. Moreover, the length-independent excitation gap *does not vanish* in the region $0 < V < V_c$, so the ground state is non-degenerate and the ladder is **not in a CDW phase**. In this region, of course, the ladder is also **non-conductive** because the energy gap is not zero. In the range $0 < V < V_c$, the ladder seems to be a **correlated band insulator**. The lowest excitation here cannot be determined from the single-particle gap or excitation gap. It could be a **bound particle-hole pair** (exciton) with binding energy $E_p - \Delta E$ or a **collective excitation** where the **C**harge **D**ensity **W**ave is not a ground state but the lowest excited state.[16–18] In order to find out exactly what kind of excitation we are dealing with here, further observables have to be

calculated, such as dynamic correlation function. This region of the interaction potential of the 1221 ladder can be investigated in more detail in a further work.

Finite-size scaling $E_p(1/L)$ of the single-particle gap as a function of $1/L$ yields the exponent $|\kappa|$ using the **P**hase **I**ndependent **F**it method. This exponent is plotted in Figure 4.9 as a function of V and shows **a sharp peak at $V_c = 2.04$** for a 1221 ladder *with* CCS and is otherwise zero in both phases as in the case of the previously investigated observables. The ladder *without* CCS has a maximum at $V_c = 2.12$ and drops to zero much more slowly (but neither exponential nor like a power law) after the phase transition. Only starting at $V \approx 4$ the exponent becomes $|\kappa| < 10^{-3}$.

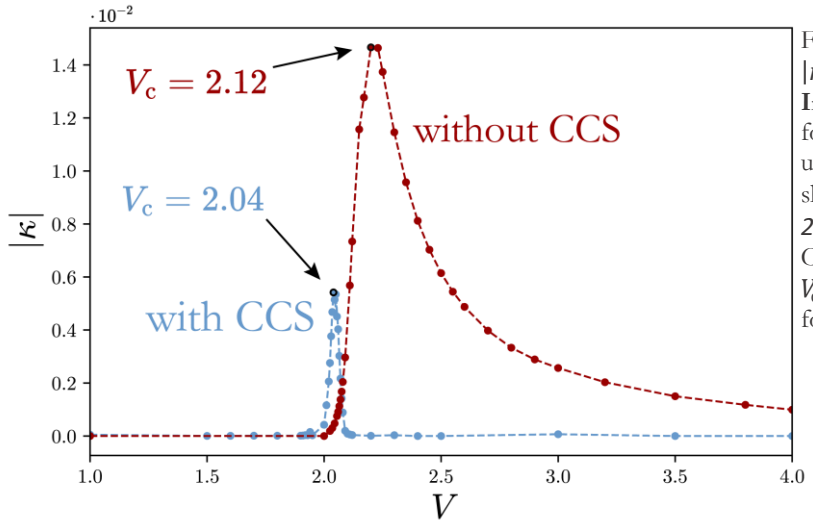

Figure 4.9: The exponent $|\kappa(V)|$ from the **P**hase **I**ndependent **F**it method for a 1221 ladder with CCS using single-particle gap shows a maximum $V_c = 2.04$ and the ladder without CCS has a maximum at $V_c = 2.12$. Dashed line is for eye-guidance.

Table 4.2 summarizes the determined critical values obtained using the single-particle gap. They agree well with the previously determined critical values.

Method	CCS	V_c
Extremum in E_p of a **F**inite **S**ystem	Yes	2.05 ± 0.05
Extremum in E_p of a **F**inite **S**ystem	No	2.22 ± 0.05
Phase **I**ndependent **F**it	Yes	2.04 ± 0.005
Phase **I**ndependent **F**it	No	2.12 ± 0.05

Table 4.2: Methods for determining the possible critical value in a 1221 chain applied to single-particle gap.

4.4. CDW ORDER PARAMETER

The **CDW order parameter** $|\delta(V)|$ is THE observable par excellence with which the CDW phase can be detected. This is because only in the CDW phase, the order parameter

is nonzero and theoretically approaches $|\delta(V)| = 0.5$ for $V \to \infty$. This behavior has been observed even in a *finite* 1DSF chain (see Figure 2.18) and in a *finite* 2-leg ladder (see Figure 3.6). The inset of Figure 4.10 confirms this behavior for $V \to \infty$ also for a *finite* 1221 ladder. From the *length independence* of the order parameter $|\delta(V)|$ for large V, it can also be concluded that also in the thermodynamic limit the order parameter of the 1221 ladder converge to $|\delta(V)| = 0.5$ with an accuracy of 0.09%. The 1221 ladder can be fitted with a 2nd degree polynomial (1.18) starting at $V > 4$. Thus, the 1221 ladder shows the same behavior as the theoretical behavior of a 1DSF chain for large interaction potentials.[3]

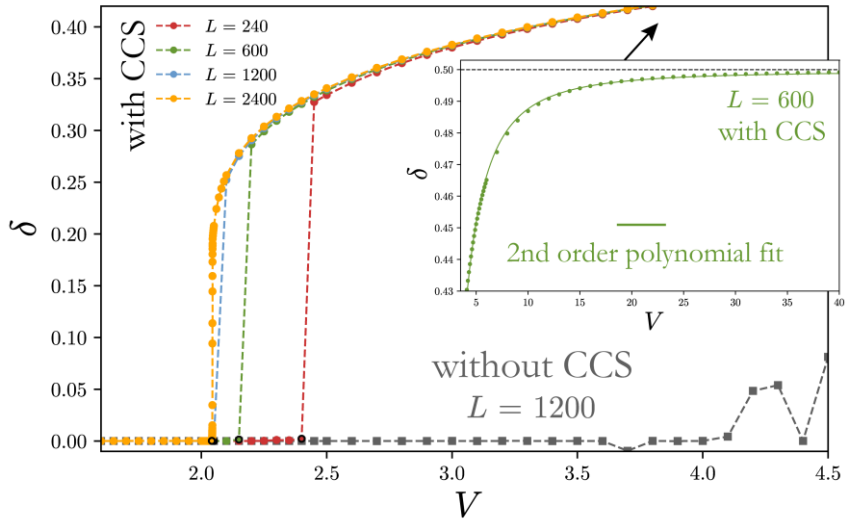

Figure 4.10: Magnitude $|\delta(V)|$ of the order parameter of a 1221 ladder with CCS shows a length dependent discontinuity near $V = 2$. The ladder without CCS is zero everywhere. The inset shows the order parameter for large V.

Furthermore, the order parameter $|\delta(V)|$ of the 1221 ladder shows the following behavior as a function of V:

- **With CCS** there is a *length dependent* (within the given accuracy: a *discontinuous*) jump from zero to a finite value. The first jump in the value of $|\delta(V)|$ (coming from small V) is extrapolated as follows: The interaction potential $V_c(1/L)$ at which this jump happens is plotted as a function of 1/L and extrapolated *linearly* to $1/L = 0$. The extrapolated critical value for a ladder in the thermodynamic limit is $V_c(0) \approx 2.01$ (see Figure 4.11).
- **Without CCS**, the order parameter $|\delta(V)|$ vanishes for all ladder sizes up to $L = 2400$ in the region $V \leq 4$. This indicates that the order parameter of a 1221 ladder *without* CCS is not a good parameter for the predictions in the thermodynamic limit.

Unfortunately, the **P**hase **I**ndependent **F**it method does not work here in the vicinity of the $V \approx 2$ phase transition because of the limited accuracy and very steep slope. Nevertheless, the **CDW order parameter** (*with* CCS) also **yields a critical value** $V_c \approx 2.01$, which agrees well with the results of previously studied observables. Moreover, the order parameter **confirms the transition to a CDW phase**.

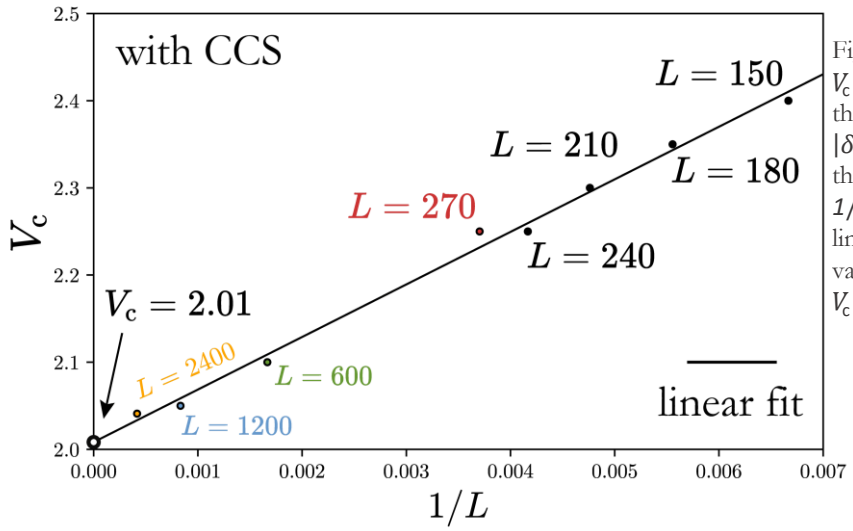

Figure 4.11: Position $V_c(1/L)$ of the jump in the order parameter $|\delta(V)|$ as a function of the inverse ladder size $1/L$ is extrapolated linearly. The critical value for $1/L = 0$ is $V_c \approx 2.01$.

The study of the CDW order parameter (*with* CCS) has confirmed that a phase transition happens near $V = 2$ **to the CDW phase**. However, the order parameter in Figure 4.10 also shows that the **size of the discontinuity** at $V_c(L)$ decreases with a larger number L of sites. The investigation of this size of discontinuity as a function of L is, however, difficult, as for example $L = 2400$ case shows. For this, the discontinuity is resolved more precisely and as can be seen, the size of the discontinuity becomes smaller as the resolution becomes larger. This implies **a second order phase transition**. However, it cannot be excluded that the magnitude of the discontinuity is very small.

4.5. Density Fluctuation

The **density fluctuation** $\sigma^2(V)$ as a function of V is another way to detect a CDW phase. In the CDW phase, $\sigma^2(V) \to 0.25$ goes for $V \to \infty$. This behavior has been observed in a *finite* 1DSF chain (see Figure 2.20) and in a *finite* 2-leg ladder (see Figure 3.7). This behavior can also be confirmed for a 1221 ladder *with/without* CCS for $V \to \infty$. The density fluctuation $\sigma^2(V)$ for $V > 4$ can be fitted with the 2nd degree polynomial (1.18) as in the case of the 1DSF chain and the 2-leg ladder. The obtained limit value differs only by 0.07% from the theoretical limit $\sigma^2(V \to \infty) = 0.25$.

As Figure 4.12 shows, density fluctuation $\sigma^2(V)$ of a 1221-ladder *with* CCS as a function of V has a **length-dependent discontinuity** that converges to the value $V_c \approx 2.01$ for $1/L \to \infty$ by using linear extrapolation (done in the same way as in Figure 4.11). The density fluctuation $\sigma^2(V)$ of a 1221 ladder *without* CCS, on the other hand, is **continuous in the critical region** and therefore cannot be used directly to determine the critical value. In contrast to the CDW order parameter, densitiy fluctuation is non-zero for $V > V_c$ and indicates that in the thermodynamic limit the 1221 ladder *without* CCS is also in the CDW phase for $V > V_c$.

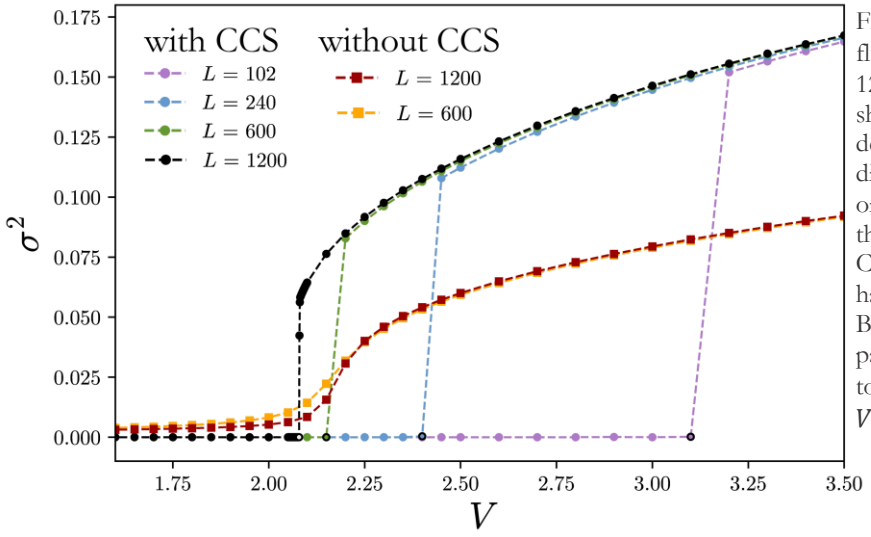

Figure 4.12: Density fluctuation σ^2 of a 1221 ladder with CCS shows a length dependent discontinuity. The order parameter of the ladder without CCS, on the other hand, is continuous. Both order parameters converge toward $\sigma^2 = 0.25$ for $V \to \infty$.

4.6. Density-density correlation function

Let's give the **density-density correlation function** $|F(x)|$ one last chance (if you haven't read the previous chapters: The correlation function is the observable that gave me the most headaches). Figure 4.13 shows $|F(x)|$ of a 1221 ladder of size $L = 600$ *with/without* CCS with reference point $x_0 = 1$. It is shown on a logarithmic scale and exhibits the following behavior:

- For a 1221 ladder *with* CCS, the correlation function decays rapidly **exponentially** with a small distance to the boundary site x_0. This behavior is typical for a band insulator.[16] However, the exponential decay is also observed in the previously determined CDW phase starting at $V \gtrsim 2$. This contradicts the previous results. The correlation function near the phase transition at $V \approx 2$ is also interesting.

Here $|F(x)|$ also decreases exponentially (with a sufficient distance to the boundary site), but *much slower*.

- A 1221 ladder *without* CCS (inset of Figure 4.13) shows something different. In the postulated CDW phase $V \gtrsim 2$, the correlation function decays exponentially only near the boundary site x_0 and **saturates at a small value** $|F(x)|$ of order 10^{-5}. However, the value is so small that the interpretation of the results is not really meaningful. If this saturation can be taken seriously, then the correlation function of a ladder without CCS with its different behavior for $V \gtrsim 2$ and $V < 2$ confirms that the ladder may have two different phases with a phase transition at $V \approx 2$.

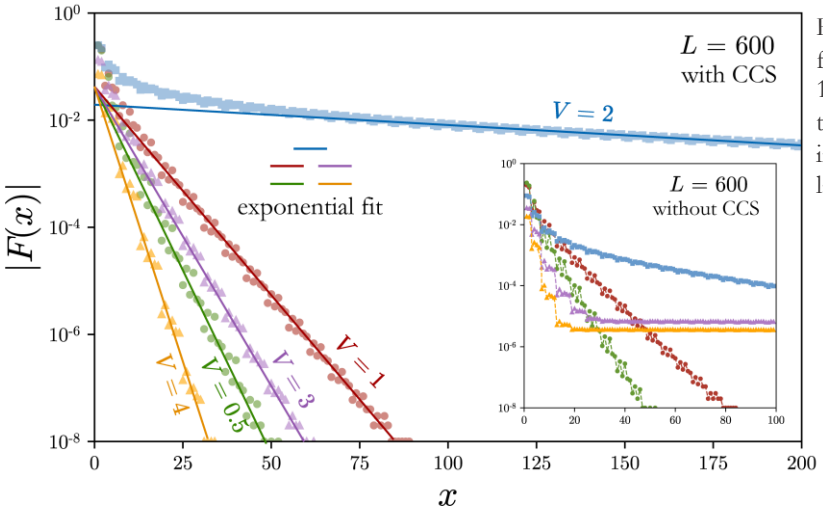

Figure 4.13: Correlation function $|F(x)|$ of a 1221 ladder with CCS of the size $L = 600$. The inset shows $|F(x)|$ of a ladder without CCS.

4.7. SUMMARY

In contrast to the 1DSF chain and 2-leg ladder, *all* observables (except correlation function) of a 1221 ladder have revealed a phase transition near $V = 2$. For a ladder *with* CCS, the entropy S and central charge c even revealed the phase transition in the form of a (numerical) discontinuity!

The excitation gap ΔE and single-particle gap E_p confirmed that for $V = 0$ the 1221 ladder is a band insulator. For $0 < V < V_c$, the excitation gap and single-particle gap were not identical and excitation gap was not zero. This could be an indication of a new *insulating* phase that is neither band insulator nor CDW phase. ΔE and E_p also provided evidence that starting **at the critical value** $V_c \leq V$ **the CDW phase begins**, because here

$\Delta E = 0$ and E_p is proportional to V, as it is in the CDW phase of the 1DSF chain and the 2-leg ladder.

CDW order parameter δ and density fluctuation σ^2 (at least for a ladder *with* CCS) clearly demonstrated that a **phase transition to the CDW phase happens at V_c** and **persists for all investigated $V \geq V_c$**.

Moreover, it has been shown that a **1221-ladder *with* CCS symmetry is better for studying phase transitions** in the thermodynamic limit because 6 out of 7 observables (except correlation function) have shown a discontinuity or extremum at the **phase transition at $\overline{V_c} = 2.04 \pm 0.07$**. Here $\overline{V_c}$ is the mean with standard deviation of all determined critical values V_c from Table 4.3.

Observable	Method	V_c
S	Linear Fit of **E**xtrema in a **F**inite **S**ystem	≈ 2.05
S	**P**hase **I**ndependent **F**it	2.05 ± 0.01
c	**E**xtremum in a **F**inite **S**ystem	2.07 ± 0.01
ΔE	**D**iscontinuity in a **F**inite **S**ystem	2.05 ± 0.05
ΔE	**P**hase **I**ndependent **F**it	2.07 ± 0.01
E_p	**E**xtremum in a **F**inite **S**ystem	2.05 ± 0.01
E_p	**P**hase **I**ndependent **F**it	2.04 ± 0.01
δ	Linear Extrapolation of **D**iscontinuity in a **F**inite **S**ystem	≈ 2.01
σ^2	Linear Extrapolation of **D**iscontinuity in a **F**inite **S**ystem	≈ 2.01

Table 4.3: All observables of a 1221 ladder **with** CCS and the applied methods that revealed a phase transition near $V = 2$.

The ladder *without* CCS worked only for 3 of 7 studied observables. These are listed in Table 4.4. The mean of the critical value $\overline{V_c} = 2.17 \pm 0.09$ is slightly higher than the mean obtained for the 1221 ladder *with* CCS symmetry. The latter should be clearly preferred, going by the number of successful observables and methods.

Observable	Method	V_c
S	Linear Fit of **E**xtrema in a **F**inite **S**ystem	≈ 2.15
S	**P**hase **I**ndependent **F**it	2.21 ± 0.01
c	**E**xtremum in a **F**inite **S**ystem	2.17 ± 0.01
E_p	**E**xtremum in a **F**inite **S**ystem	2.22 ± 0.05

Observable	Method	V_c
E_p	**P**hase **I**ndependent **F**it	2.12 ± 0.05

Table 4.4: All observables of a 1221 ladder **without** CCS and the applied methods that revealed a phase transition near $V = 2$.

Conclusion

In this work, quantum phases and the transition between phases in three spinless fermionic systems were studied using **D**ensity **M**atrix **R**enormalization **G**roup algorithm. The 1DSF chain and 2-leg ladder with theoretically known exact **C**harge **D**ensity **W**ave phase transitions at $V_{\mathrm{cdw}} = 2$ (1DSF) and $V_{\mathrm{cdw}} = 0$ (2-leg) served as toy models on which various numerical methods for determining these critical values were tested. They were then applied to a less known system, the 1221 ladder. The study of these systems has revealed **5 important points**:

1. Some observables $O(V)$ as a function of the interaction potential V *directly* **exhibit an extremum** that is close to the exact phase transition.
2. Some observables, on the other hand, can only be used *indirectly* to determine the critical value by **applying a suitable method**. From the entropy $S(V)$ of a 1DSF chain as a function of V, for example, a phase transition cannot be obtained directly, but by using the **P**hase **I**ndependent **F**it method in combination with the power law, the phase transition in the thermodynamic limit can be revealed very accurately.
3. In most cases it is **not necessary to choose a large dimension** $m > 100$ of the Hilbert space of the left block for DMRG to investigate phase transitions quantitatively (at least for the 1DSF chain and 1221 ladder). This saves computing power and time. However, one still has to be careful because by choosing too small m one can reach a different ground state in Hilbert space.
4. Systems *with* **C**harge **C**onjugation **S**ymmetry described by Hamiltonian (1.9) **work better** in determining the phase transitions. There were more observables and methods that worked.
5. The **P**hase **I**ndependent **F**it method in combination with the power law provided an accurate critical value for both the 1DSF chain and the 1221 ladder. It was the only method that could be used across systems and observables.

Surprisingly, in the case of the at least theoretically known system, the 1221 ladder, most of the observables and methods worked! Thus, it was possible to detect **a phase transition at** $V_c = 2.04 \pm 0.07$ from an insulating phase to the insulating CDW phase. However, what remains unclear is what phase is in the region between the band insulator $(V = 0)$ and CDW phase $(V = V_c)$. Some guesses were made in Chapter 4.3. However, the problem must be investigated in more detail.

The author ventures another *guess* concerning the determined critical point V_c: Is nature really so brutal and would choose a phase transition of a half-filled infinite 1221 ladder at such an ugly value as 2.04? The author assumes that the **phase transition value** $V_{cdw} = 2$ of the 1DSF chain **does not change upon transformation to a 1221 ladder**. This assumption could be checked by a clever theorist.

During the course of this work, **5 additional problems** arose that were not resolved and should be investigated in more detail in future work:

1. There seems to be a relationship between the theoretical central charge c of the 1DSF model and the exponent $|\kappa|$ from the **P**hase **I**ndependent **F**it method. Both are $|\kappa| = c = 0$ in an *insulating* phase and both $|\kappa| = c = 1$ in a *metallic* phase. Are these quantities related?
2. Which insulating phase of the 1221 ladder is located in the region between the band insulator $(V = 0)$ and CDW phase $(V = V_c)$?
3. Where is the exact theoretical phase transition V_{cdw} in the thermodynamic limit for the 1221 ladder?
4. The **P**hase **I**ndependent **F**it method has worked system-wide and successfully revealed phase transitions in the thermodynamic limit. To which other quantum systems with known and unknown phase transitions can the method be successfully applied?
5. How can the author get rid of his headache caused by the density-density correlation function $|F(x)|$?

References

1. Giamarchi, T. *Quantum physics in one dimension* (Clarendon Press, Oxford, 2004).
2. Gaudin, M. *The Bethe wavefunction* (Cambridge University Press, Cambridge, 2014).
3. Gebhard, F., Bauerbach, K. & Legeza, Ö. Accurate localization of Kosterlitz-Thouless-type quantum phase transitions for one-dimensional spinless fermions. *Phys. Rev. B* **106**; 10.1103/PhysRevB.106.205133 (2022).
4. Abdelwahab, A. & Jeckelmann, E. Luttinger liquid and charge-density-wave phases in a spinless fermion wire on a semiconducting substrate. *Phys. Rev. B* **98**; 10.1103/PhysRevB.98.235138 (2018).
5. Abdelwahab, A., Jeckelmann, E. & Hohenadler, M. Correlated atomic wires on substrates. I. Mapping to quasi-one-dimensional models. *Phys. Rev. B* **96**; 10.1103/PhysRevB.96.035445 (2017).
6. Abdelwahab, A. & Jeckelmann, E. Effective narrow ladder model for two quantum wires on a semiconducting substrate. *Phys. Rev. B* **103**; 10.1103/PhysRevB.103.245405 (2021).
7. Schollwöck, U. The density-matrix renormalization group in the age of matrix product states. *Annals of Physics* **326,** 96–192; 10.1016/j.aop.2010.09.012 (2011).
8. Montangero, S. *Introduction to tensor network methods. Numerical simulations of low-dimensional many-body quantum systems* (Springer, Cham, 2018).
9. Malvezzi, A. L. An introduction to numerical methods in low-dimensional quantum systems; 10.48550/arXiv.cond-mat/0304375 (2003).
10. Jeckelmann, E. Density-matrix renormalization group algorithms. In *Computational Many-Particle Physics* (Springer2008), pp. 597–619.
11. Donohue, P., Tsuchiizu, M., Giamarchi, T. & Suzumura, Y. Spinless fermion ladders at half filling. *Phys. Rev. B* **63**; 10.1103/PhysRevB.63.045121 (2001).

12. Essalah, K., Benali, A., Abdelwahab, A., Jeckelmann, E. & Scalettar, R. T. Magnetic properties of alternating Hubbard ladders. *Phys. Rev. B* **103**; 10.1103/PhysRevB.103.165127 (2021).

13. Nishimoto, S. Tomonaga-Luttinger-liquid criticality: Numerical entanglement entropy approach. *Phys. Rev. B* **84**; 10.1103/PhysRevB.84.195108 (2011).

14. Fehske, H., Schneider, R. & Weiße, A. (eds.). *Computational Many-Particle Physics* (Springer Berlin Heidelberg, Berlin, Heidelberg, 2007).

15. Schmitteckert, P. & Eckern, U. Phase Coherence in a Random One-Dimensional System of Interacting Fermions: A Density Matrix Renormalization Group Study; 10.48550/arXiv.cond-mat/9604005 (1996).

16. Jeckelmann, E., personal communication.

17. Sólyom, J. *Fundamentals of the physics of solids* (Springer, Berlin, 2007).

18. Sólyom, J. *Fundamentals of the Physics of Solids. Volume 3 - Normal, Broken-Symmetry, and Correlated Systems* (Springer-Verlag Berlin Heidelberg, Berlin, Heidelberg, 2010).